

AUS DEM LEHRSTUHL FÜR NEUROLOGIE
DIREKTOR: PROF. DR. U. BOGDAHN
DER FAKULTÄT FÜR MEDIZIN
DER UNIVERSITÄT REGENSBURG

Myeloid-derived Suppressor Cells in Glioblastoma Patients -
Phenotype, Function and Clinical Relevance

Inagural-Dissertation
zur Erlangung des Doktorgrades
der Medizin

der
Medizinischen Fakultät
der Universität Regensburg

vorgelegt von
Daniel Dubinski M.Sc.

2016

„Its palliation is a daily task, its cure a fervent hope.“
-William Castle, 1950

This work was partially published in: Neuro-Oncology 2015 Nov 17. Pii:nov280

Dekan:

Prof. Dr. Dr. Torsten E. Reichert

1. Berichterstatter:

Priv.-Doz. Dr. Dr. Oliver Grauer

2. Berichterstatter:

Prof.Dr. Peter Hau

Tag der mündlichen Prüfung:

Table of contents

1. Introduction.....	6
1.1 Clinical aspects of Glioblastoma (incidence, diagnosis, treatment)	6
1.1.1 Incidence	6
1.1.2 Diagnosis.....	7
1.1.3 Treatment.....	9
1.2. Immune System	12
1.2.1 Basics of the human immune system (innate/acquired)	12
1.2.1 Antigen-presentation and the major histocompatibility complex	14
1.2.3 T-Cells.....	15
1.2.4 The Immune System in the CNS.....	17
1.2.5 Tumor immunology in GBM	18
1.3 Myeloid Derived Suppressor Cell's	18
1.3.1 Characteristics.....	18
2. Aim of this thesis.....	22
3. Material and Methods	23
3.1 Material	23
3.1.1 Disposable materials	23
3.1.2 Chemicals and reagents	23
3.1.3 Kits	24
3.1.4 Media, reagents and supplements for cell culture.....	24
3.1.5 Antibodies	25
3.1.6. Buffer	26
3.2 Methods.....	26
3.2.1 Patients characteristics.....	26
3.2.2 Intraoperative CUSA assisted resection of GBM	26

3.2.3	Isolation of tumor infiltrated leucocytes (TIL's) from tumor-tissue	27
3.2.4	Isolation of peripheral blood mononuclear cell's (PBMC) from venous blood 28	
3.2.5	Fluorescent activated cell sorting (FACS).....	28
3.2.6	Cytospin preparation.....	28
3.2.7	ROS detection	29
3.2.8	Arginase detection	29
3.2.9	MRI scans and tumor volume measurement.....	30
3.2.10	T-cell proliferation assay	30
3.2.11	Intracellular INF- γ detection.....	31
3.2.12	Statistic	31
4.	Results	32
4.1	Phenotype, morphology and frequency of different MDSC subsets in peripheral blood and tumor tissue of primary glioblastoma patients	32
4.2.	Patients characteristic n=52.....	33
4.3	Morphologic characteristics of different MDSCs subsets.....	34
4.4	Distribution of different MDSCs subsets within PBMC and TILs of healthy donors (HD) and glioblastoma patients (GBM).....	36
4.5	Phenotypic analysis of MDSC subpopulation in peripheral blood and tumor 38	
4.6	Influence of steroid ingestion and MGMT status on MDSCs subgroups	39
4.7.	DCFA and ARG1 expression of MDSC subpopulation in PBMCs and TILs in GBM	40
4.8	T-cell suppression assay of sorted MDSC subpopulations	42
4.9.	Frequency of MDSC in tumor is dependent on tumor volume	43
4.10	MDSC correlationwith time to tumor progression and Treg presence....	44
5.	Discussion	47
6.	Summary	51

7. Zusammenfassung	52
8. References	53

List of tables

Table 1: The World Health Organization (WHO) grading system for astrocytoma (adapted from [4])	7
Table 2: Disposable materials	23
Table 3: Chemicals and reagents	23
Table 4: Kits.....	24
Table 5: Media, reagents and supplements for cell culture.....	24
Table 6: Antibodies.....	25
Table 7: Buffer.....	26
Table 8: Patients characteristic n=52.....	33
Table 9: Distribution of different MDSCs subsets within PBMC and TILs of healthy donors (HD) and glioblastoma patients (GBM).....	36

List of figures

Figure 1: MRT-morphology of left frontal GBM: (adapted from [5]) A: Axial view shows a hypointense lesion B: T1 post contrast image with irregular enhancement. C: T2 FLAIR images show increase in FLAIR signal. D: T2 FSE images also demonstrate increase in signal	8
Figure 2: Kaplan-Maier estimates of overall survival by treatment group (adapted from [10]).	10
Figure 3: MGMT is inhibiting temozolomide therapy (adapted from [12])	11
Figure 4: Overall survival according to MGMT promoter methylation in combined radiochemo therapy vs radiotherapy alone. A:Patients with methylated MGMT promoter. B: Patients with unmethylated MGMT promoter (adapted from [10]).....	12
Figure 5: Four basic principles of T-cell suppression through Tregs (adapted from [15])	17
Figure 6: Presence of myeloid derived suppressor cells in human diseases (adapted from [31])	21
Figure 7: Mechanisms of MDSC mediated immune suppression. (adapted from [39])	22
Figure 8: left: intraoperative view of Glioblastoma resection situs with the CUSA apparatus, right: laboratory setting before proceeding the specimen	27
Figure 9: Gating strategy for the assessment of the MDSC population from tumor infiltrating leucocytes and periphery blood mononuclear cells, using flow cytometry in GBM patients. A: Cells obtained from tumor tissue. B: Cells obtained from peripheral blood.....	33
Figure 10: Morphologic characteristics of different MDSC subsets in the peripheral blood of glioblastoma patients.-Myeloid cells were labeled with anti-CD11b and anti-CD14 antibodies and after sorting four major MDSC subpopulations were defined: CD14 ^{high} CD15 ^{positive} are further referred to as a monocytic phenotype, CD14 ^{low} CD15 ^{low} MDSCs showed characteristics of immature myeloid cells and the CD14 ^{low} CD15 ^{positive}	

granulocytic phenotype consisted of CD14^{low}CD15^{high} neutrophils and CD14^{low}CD15^{intermediate} eosinophils..... 35

Figure 11: shows different subtype distributions of MDSCs in GBM patients. Healthy donors N=26, GBM N=52. 35

Figure 12: Phenotypic analysis of monocytic, granulocytic, neutrophilic and eosinophilic MDSCs in peripheral blood (PBMC), tumor specimen (TIL) and healthy donors (HD)..... 38

Figure 13: MDSC distribution in the tumor and peripheral blood with and without steroid ingestion 39

Figure 14: MDSC distribution in the tumor and peripheral blood according to MGMT promoter methylation status 40

Figure 15: Arginase 1 (Arg1+) and ROS (DCFA+) expression of the four different subtypes obtained from peripheral blood and tumor..... 41

Figure 16: FACS analysis and CFSE distribution after performance of T-cell suppression assay 42

Figure 17: Representative dot plots of T cell proliferation and intracellular INF- γ secretion after addition of neutrophilic MDSCs to CFSE-labeled autologous T-cells and PMA/ionomycin stimulation..... 43

Figure 18: Correlation between the proportion of granulocytic, neutrophilic, eosinophilic and monocytic MDSCs within TILs (n=52) and the tumor volume before tumor resection..... 44

Figure 19: Representative dot plot for neutrophilic and monocytic TIL and PBMC MDSC subpopulation (n=39). No significant correlation between MDSC in peripheral blood and at the tumor site was found 45

Figure 20: Representative dot plot for granulocytic (CD14^{low}CD15^{positive}) TIL and PBMC MDSC and monocytic (CD14^{high}CD15^{positive}) TIL and PBMC (n=28). No significant correlation between MDSC in peripheral blood or at the tumor was found to correlate with time to progression..... 46

1. Introduction

1.1 Clinical aspects of Glioblastoma (incidence, diagnosis, treatment)

1.1.1 Incidence

Among all cancers, glioblastoma multiforme (GBM) is the most frequent and most malignant human brain tumor. GBMs are very aggressive, highly invasive as well as neurologically destructive. They are considered to be among the deadliest of human cancers, with median survival from 9 to 12 months on average. GBM typically originates in the cerebral hemisphere of patients between 50 and 70 years of age from a differentiated astrocyte or brain tumor-initiating cell (BTIC), preferably within the white matter of the frontal, temporal, or parietal lobe. Of the estimated 2000-3000 primary brain tumors diagnosed in Germany each year, approximately 70% are GBM. The incidence for GBM is therefore 5 cases per 100000 patients [1,2].

Glioblastomas are divided into two subclasses based on clinical characteristics: primary and secondary GBMs. Primary GBMs, found more frequently in older patients, are very aggressive and highly invasive. They arise from a de novo process, in the absence of a preexisting low-grade lesion. Secondary GBMs are usually observed in younger patients and develop progressively from low-grade astrocytoma over a period of 5 to 10 years [3].

The World Health Organization (WHO) grading system classifies gliomas into grade I to IV based on their degree of malignancy, as determined by histopathological criteria [4]. Table 1 displays examples and the criteria according to the WHO classification system. In the year 2016 a new WHO grading system will be introduced but is not available by the time of writing. In the central nervous system grade I gliomas generally originate in a benign way, are circumscribed, median survival is higher and curative approaches are possible. Grade II-IV gliomas are malignant and diffusely infiltrate throughout the brain making a curative approach often impossible. Astrocytomas are the most common CNS neoplasms, representing more than 60% of all primary brain tumors. They vary from grade II to III. Glioblastoma multiforme is the most malignant form of infiltrating astrocytoma and is classified as grade IV astrocytoma. It is known to be one of the most aggressive human cancers.

Table1: The World Health Organization (WHO) grading system for astrocytoma (adapted from [4])

WHO-Grade	Example	Criteria
WHO-Grade I	Pilocytic astrocytoma, Ependymoma/Subependymoma	Low proliferating, discrete, non-invasive character
WHO-Grade II	Diffuse astrocytoma, papillary-, cellular- and clear cell ependymoma	Modestly proliferating, partly invasive character
WHO-Grade III	Anaplastic astrocytoma/ Anaplastic ependymoma	Fast proliferating, invasive character
WHO-Grade IV	Glioblastoma multiforme, Medulloblastoma, highly malignant glioma-like Pineoblastoma	Rapidly proliferating, highly invasive character, necrosis

1.1.2 Diagnosis

Along with a history of present disease and a neurological examination the radiographic appearance is the first evidence of a glioblastoma burden. GBMs are known for rapid cell turnover, which leads to an insufficient vascular supply. The typical radiographic correlation to this fact is a ring-enhanced lesion with a necrotic core, a large amount of vasogenic edema and a mass effect in the appearance on MRI. In the CT scan, GBM impresses as a space-occupying lesion with an irregular hypodense center representing necrosis. It can present with a midline shift or a compression of ventricles. In the T1 section, glioblastoma presents as a hypo- to isointense mass within the white matter containing a central heterogeneous signal representing necrosis and intratumoral hemorrhage. The enhancement is variable, typically peripheral and irregular. In the T2 and FLAIR section, the tumor shows a hyperintense mass surrounded by vasogenic edema. PET scans can show an accumulation of FDG (representing increased glucose metabolism), which typically is greater in the tumor than in the physiological metabolism of the gray matter. The

typical radiographic appearance of a left frontal glioblastoma in the different sequences is shown in Figure 1.

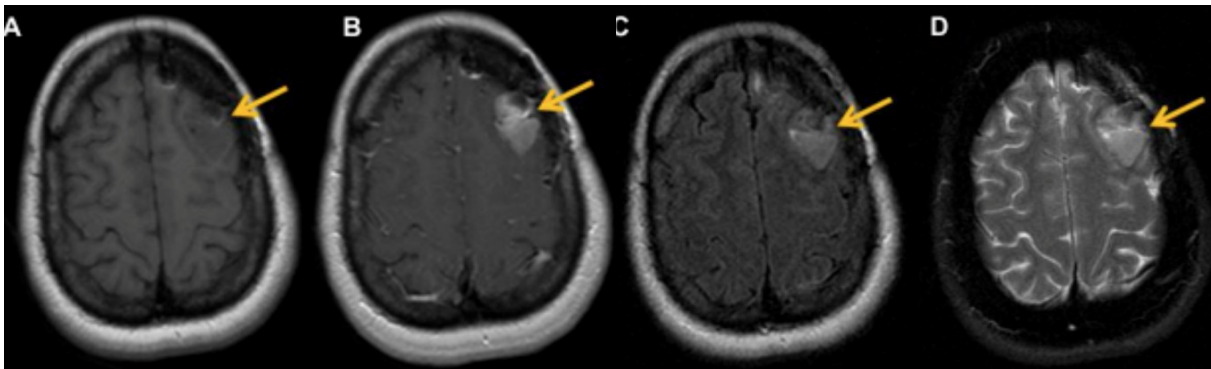


Figure 1: MRT-morphology of left frontal GBM: (adapted from [5]) A: Axial view shows a hypointense lesion B: T1 post contrast image with irregular enhancement. C: T2 FLAIR images show increase in FLAIR signal. D: T2 FSE images also demonstrate increase in signal

The differential diagnosis for a ring-enhanced lesion on MRI includes besides tumor: abscess, metastasis, brain lymphoma, demyelination and subacute ischemia. Therefore a definitive diagnosis of a suspected GBM on a CT or MRI scan can be proven only by a stereotactic biopsy or craniotomy with tumor resection followed by a histopathological examination. After the neuropathological diagnosis, the patient's treatment can be initiated.

Surgery in malignant glioma patients commonly aims at removing as much of the tumor as possible without causing new neurological deficits in the patient. Biopsy may be the only option for multifocal tumors, tumors involving the corpus callosum or other eloquent regions. Although a total resection cannot be achieved in glioma surgery at present, the benefits of a glioma surgery contain: symptomatic relief from a mass effect and obstructed cerebrospinal fluid (CSF) circulation. After surgical relief of local compression, global symptoms such as headache, nausea and vomiting can improve along with a reversal of neurological deficits [6]. Another benefit of aggressive surgical resection is the reduction in the amount of neoplastic cells. A lower tumor load increases the efficacy of adjuvant therapy [7]. A further profit of a neurosurgical intervention is the more accurate diagnosis. The accuracy of histological diagnosis is dependent on the size of the tissue sample. False negative diagnosis is often related to a stereotactic biopsy as a result of limited tissue

samples[8]. Another notable benefit is the collection of human tumor samples for research analysis such as has been performed for this thesis.

In order to maximize the removal of pathological tissue with the minimum post-operative functional deficit the pre-operative knowledge of the proximity of the pathological tissue to the eloquent cortex is of fundamental importance for accurate and safe neurosurgical planning. Functional MRI provides information regarding anatomical variations, as well as a tumor related shift of functional cortical centers. Recently, the use of 5-ALA(5-Aminolevulinic acid)was established in glioma surgery. 5-ALA induces the accumulation of fluorescent porphyrins selectively in glioma cells. The dye is orally applied in a dosage of 20mg/Kg 5 hours prior to surgery. During operation the tumor can be visualized under dark light condition. More complete resections can be achieved which prolongs patients survival [9]. However, a complete tumor resection (R=0) can not be guaranteed and chemotherapy is part of the treatment protocol.

1.1.3 Treatment

The current treatment for newly diagnosed GBM includes surgical resection, followed by radio-chemotherapy with temozolomide (TMZ). This is based on the investigation of the European Organization for Research and Treatment of Cancer (EORTC) and the National Cancer Institute of Canada (NCIC). In 2009, Stupp et al designed a large multicenter phase III trial to compare the concurrent use of temozolomide and radiation therapy versus radiation therapy alone in patients with histologically confirmed newly diagnosed glioblastoma. The final analysis included a median follow-up of 61 months. Progression-free survival in the treatment group was 11.2% at 2 years, 6% at 3 years, 5.6% at 4 years, and 4.1% at 5 years. For patients treated with radiation alone, the progression-free survival was 1.8% at 2 years and 1.3% at 3, 4, and 5 years [10] (Figure 2).

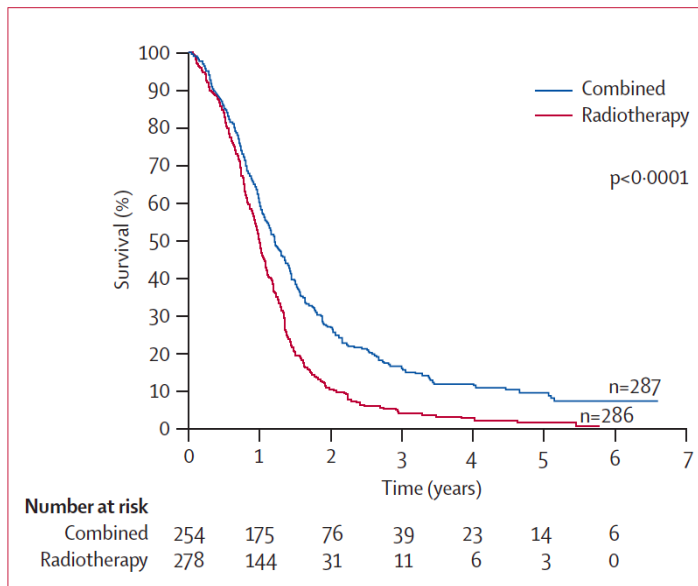


Figure 2: Kaplan-Maier estimates of overall survival by treatment group (adapted from [10]).

Particularly important in glioblastoma is the methylation status of MGMT (O-6-methylguanine-DNA methyltransferase), which is a predictive factor for therapy response and the survival of glioblastoma patients treated with temozolomide (TMZ) and radiation therapy (RT). MGMT methylation has been observed in about 35% of primary glioblastomas [11]. The methylation status of MGMT is a positive prognostic marker. It is frequently used as a diagnostic tool. TMZ and other alkylating agents modify the O6-position in guanines thereby forming critical DNA lesions that progress to lethal DNA cross-links, which prohibit cell replication. The DNA repair enzyme MGMT is able to remove alkyl groups, thus introducing resistance to TMZ treatment. When the promoter of MGMT is methylated, MGMT is not transcribed and therefore cannot repair DNA damage caused by TMZ making TMZ more efficient and prolonging overall survival. The mechanism is displayed in Figure 3.

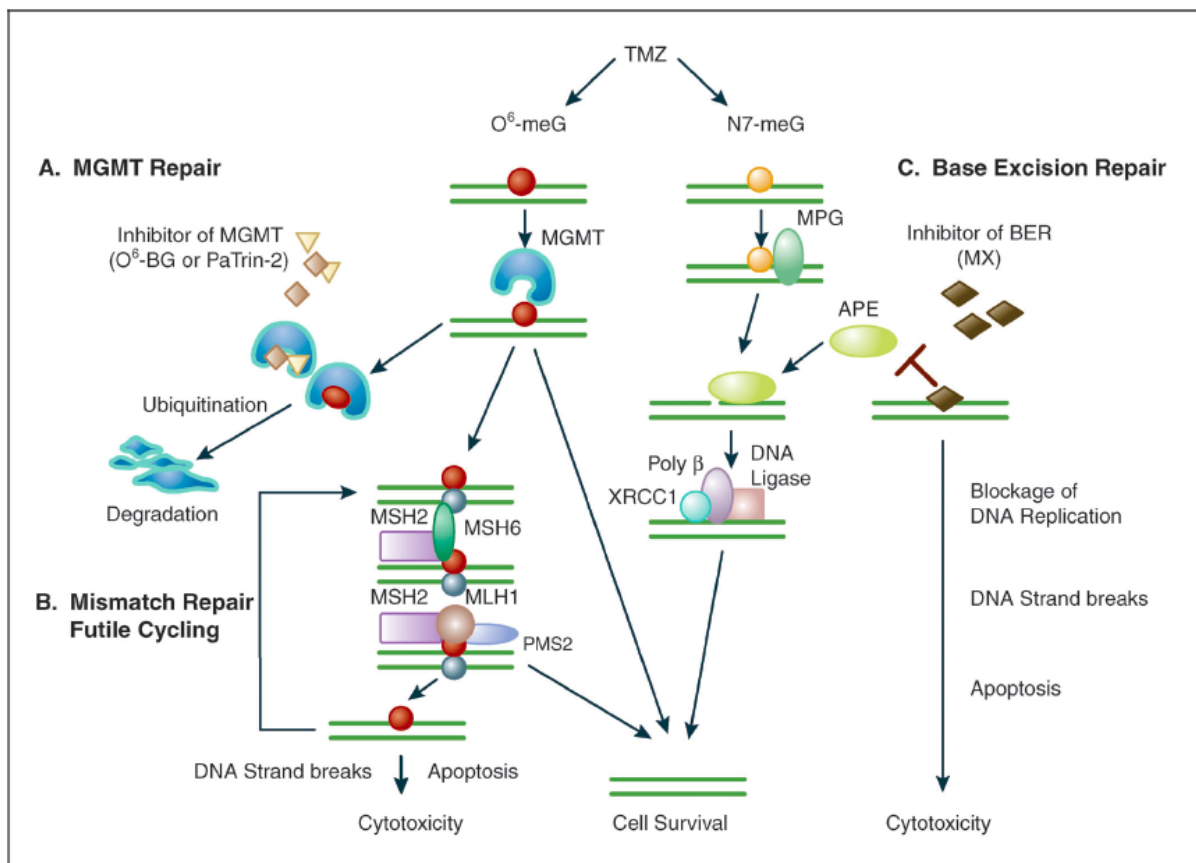


Figure 3: MGMT is inhibiting temozolomide therapy (adapted from [12])

Patients with a methylated MGMT promoter show a partial response to chemotherapy, and the overall survival is higher when compared to patients with unmethylated tumors. The lack of MGMT methylation is associated with a much higher risk of death and a lower overall survival [10]. However, the methylation status of the MGMT promoter is a better predictive factor of outcome after chemotherapy treatment than the grade of the tumor, the Karnofsky performance status or the patient's age. Kaplan-Meier curve in Figure 4 displays the difference for overall survival according to MGMT promoter methylation [10].

1.2. Immune System

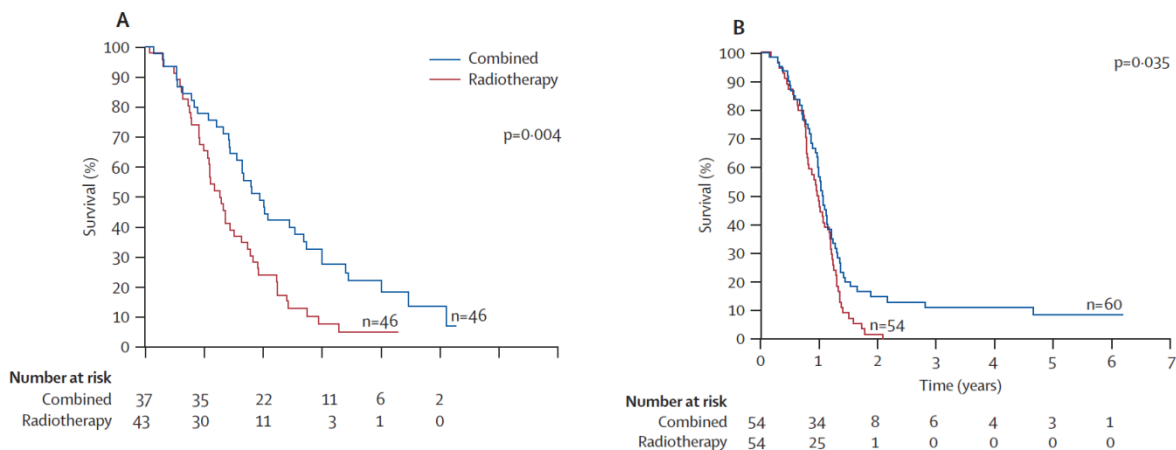


Figure 4: Overall survival according to MGMT promoter methylation in combined radiochemo therapy vs radiotherapy alone. A: Patients with methylated MGMT promoter. B: Patients with unmethylated MGMT promoter (adapted from [10])

1.2.1 Basics of the human immune system (innate/acquired)

The physiological task of the human immune system is the recognition and defense of harmful pathogens. The classical concept of the immune system distinguishes between innate and acquired immunity. Both forms contain cellular and humoral components, which are described as follows:

Characteristic for innate immunity is a general reaction against a wide spectrum of genetically conserved pathogens, an inability to modify the evolutionary preserved function and a full reactivity at the first contact with an antigen without previous sensitization. The cellular spectrum of the innate immunity consists of granulocytes and the monocyte-macrophage system, whereas the humoral spectrum contains a multitude of proteins, which are found in blood and other body fluids and can defend the organism without cellular components. Examples of these proteins are lysozyme, defensin, mannan-binding lectin, c-reactive protein, LPS-binding protein as well as a group of proteins of the complement system. The basic mechanism of action is the recognition of certain patterns which are common in several pathogens, but are absent on human cells. A good example for this pathogenic pattern is the lipopolysaccharide (LPS), which is a part of the gram-negative bacterial cell wall. Granulocytes, specially neutrophilic granulocytes are circulating in a large cell amount in the blood-system. They are migrating, mediated by chemotactic mediators

and activated endothelia, into the locus of tissue damage. Granulocytes are loaded with a diverse amount of lytic enzymes in their intracellular granula, which give them the ability to lyse cellular debris and pathogens after phagocytosis. This fast appearing first immune reaction is responsible for the stereotypical clinical presentation of inflammation: rubor, calor, dolor, and pus (as a result of degenerated granulocytes) as well as blood-neutrophilia. The granulocytic inflammation can be enhanced via the mechanism of opsonization (pathogen marking for phagocytosis) through the humoral component of the innate immune system, namely by opsonization with proteins of the complement system and the recognition through the granulocytic complement-receptors, as well as through the humoral acquired part of the immune system, namely opsonization with specific immunoglobulins and their recognition through granulocytic Fc-receptors.

Contrary to the enormous amount of circulating, short-lived granulocytes, cells of the monocyte-macrophage system are present in a smaller amount of circulating or tissue resident long-living cells which are equipped with related capabilities, but still differ in important topics. Analogous to the granulocytes, macrophages can recognize antigen-patterns and phagocyte/lyse infected structures through their membrane-bound receptors such as CD14 molecules, scavenger-receptors, mannose-receptors, complement-receptors and toll-like-receptors (TLR). An important role of the immune reaction of these cells is the activation of the acquired immune system, namely the lymphocytes. This is maintained via two main mechanisms. On the one hand, the secretion of tumor necrose-factor alpha (TNF α) and interleukin 8 (IL-8) modulates the permeability of the vessel-endothelia which enables the invasion of plasma-proteins into the inflammatory tissue region. Further the endothelia-modulation leads to restriction of the leucocytes (rolling) and facilitates the penetration of leucocytes through the vessel (extravasation), which leads to an accumulation of effector cells in the inflammatory region. On the other hand, macrophages secrete IL-6 and IL-1, which stimulates the liver to produce acute-phase-proteins (e.g. c-reactive-protein) and respectively leads to an increase of body temperature. Taken together, these mechanisms create a pro-inflammatory setting, which itself will induce further immunologic reactions described next [13].

Characteristic for the acquired or adaptive immune system is the creation of an immunologic memory, which will allow the organism to react faster and more

intensely, in the case of repeated exposure to a certain pathogen. The acquired immune system is therefore a tool which can be sensitized after a first time pathogen contact or in an iatrogenic manner such as vaccination. The cellular component of the acquired immune system consists of lymphocytes, which can be further subdivided into T-cells and B-cells. Immunoglobulins, (e.g. IgG) which are secreted by the B-cells or respectively their activated form the plasma B cells, form the humoral component of the acquired immunity.

T- and B- Cells provide a pool of resting cells which differs in the preformed antigen-specificity of their surface receptors. As a basic functional concept, T- and B-cells are activated according to their antigen-specificity after exposure of the body to the specific antigen in a phase called the initiation phase. Resting T-cells (T-helper cells or cytotoxic T-cells) are activated through dendritic cells, resting B-Cells are activated by T-effector cells. Respectively, the clonal expansion of these activated cells and their differentiation into effector cells lead to a specific immune-reaction against the corresponding antigen in a phase called effector phase.

In the case of T-cells, the main effect is a lysis of target cells through cytotoxic T-cells (CTL). The transformation from resting B-cells to activated plasma-B-cells will respectively lead to synthesis and release of specific immunoglobulins with the effect of opsonization of the target pathogen. Whereas the first antigen contact will take a long response time of the previously described signal pathway, a second exposure will lead to a much faster immunologic reaction. This can be achieved by the generation of memory-T- and B-cells, which will remain as an immunological memory after a healed up tissue damage or infection. The amount of cells containing antigen specific surface-receptors remains hereby elevated. Moreover the activation of memory cells is easier and more effectively achieved as for example naïve T-cells can be activated only via dendritic cells whereas memory-T-cells can be activated through every kind of antigen presenting cell (APC).

1.2.1 Antigen-presentation and the major histocompatibility complex

The function of the acquired immune system is based on the cleavage of endogenous as well as exogenous proteins into peptides (antigen processing) and their following presentation on the cell surface (antigen presentation). This processes

takes place in almost all human cells, although there is a difference between nucleated cells and the APCs.

In almost all nucleated cells, within the scope of cytosolic protein transport of the antigen proceeding, endogenous proteins or proteins of intracellular pathogens (virus, chlamydia, toxoplasmosis) are cleaved in the proteasome into peptides. These peptides are transferred in a ATP-dependant manner into the endoplasmic reticulum, where the peptides are associated with the major histocompatibility class I-proteins (MHC-class I proteins) and carried to the cell membrane from where they can be recognized by cytotoxic T-cells. In specialized antigen presenting cells such as dendritic cells (DC) and microglia, extern proteins can be ingested via phagocytosis or receptor mediated endocytosis. The potentially harmful proteins can further be processed for antigen presentation. After intracellular cleavage in the lysosome, the resulting peptides are associated with MHC-class II proteins for cell membrane associated presentation. T-helper cells can recognize the presentation and induce target specific cytotoxic immune response.

1.2.3 T-cells

Within the T-lymphopoiesis, multi potent lymphatic stem-cells from the bone marrow undergo an important phase of their development in the thymus. The thymus is the organ where through the mechanism of positive selection auto-reactivity of T-cells is prevented. Only T-cells which recognize the body own MHC-proteins are selected for further proceedings. The second step is known as a negative selection. Autoreactive T-cells and lymphocytes which show a reactivity against body own peptides are eliminated through induced apoptosis [13].

Due to this mechanism, the body creates a T-cell contingent which can identify exogenous peptides that are presented in association with MHC-proteins, whereas auto-antigens under physiological circumstances are recognized as endogenous and are exempt from an immune reaction. With the assistance of flow cytometry analysis, T-cells in general can be described as CD3⁺ cells within the CD45⁺ leucocyte population. A further characteristic feature of T-cells is the expression of a T-cell-receptor (TCR), which shows in analogy with the immunoglobulin's a variable

antigen-specific region. A further subdivision of CD45⁺ CD3⁺ cells can be achieved with the surfacemarkers CD4, CD8 and CD25. According to this, T-cells located in the human immune system can be subdivided as follows:

CD45⁺ CD3⁺ CD4⁺ : This subgroup consists of T-helper-cells (Th-Cells), which can recognize peptides presented on the MHC-class II proteins and after activation through antigen presenting cells (APC) can take several further differentiations:

-Th1-Cells: As effector-cells, Th1-cells can recognize their specific peptide on dendritic cells (DC) and produce IL-2 along with interferon γ (IFN γ). They induce a cellular immune reaction through activation of macrophages and cytotoxic T-cells as well as the synthesis of opsonizing immunoglobulins (IgG and IgM).

-Th2-Cells: As effectorcells, Th2-Cells recognize their specific peptide on B-cells, produce IL-4 and via B-cell activation, induce a humoral immunologic reaction including the synthesis of all kinds of immunoglobulins as well as the activation of eosinophilic granulocytes and mastcells, B-cell activation and plasmacelldifferentiation

-Th3-Cells: This subpopulation of T-cells produce IL-10 and transforming growth factor β (TGF β) and cause negative regulatory effect on the immune response.

-CD45⁺ CD3⁺ CD8⁺: These cytotoxic T-cells (CTL), recognize peptides presented on MHC-class I proteins, and after being activated induce the apoptosis of the presenting cell through secreting perforin, granzymes and FasL.

-CD45⁺ CD3⁺ CD4⁺ CD25⁺: This subgroup is termed regulatory T-cells (Treg). Tregs, after being activated through their specific TCR, can initiate a suppression of the immunologic response of all other T-cellsubtypes. Their role is essential for maintaining peripheral tolerance, preventing autoimmune diseases and limiting chronic inflammatory diseases. As a negative result, their presence seems to limit the anti-tumor immunity. According to the flow cytometric analysis of surface markers, Treg express continually the transcriptionfactor FoxP3, which is seen as a specific marker for Treg [14]. The absence of the CD127 marker on CD4⁺ CD25⁺ cells defines the characteristic of this subpopulation, as the correlation of the absence of CD127 and the presence of FoxP3 on Tregs is over 90% [12]. The mechanism of immunosuppression by Tregs is not fully understood, but includes amino acid

depletion, cytokine secretion (TGF- β , IL-10) and direct cell-cell inhibition leading to a local immunosuppressive environment (Figure 5).

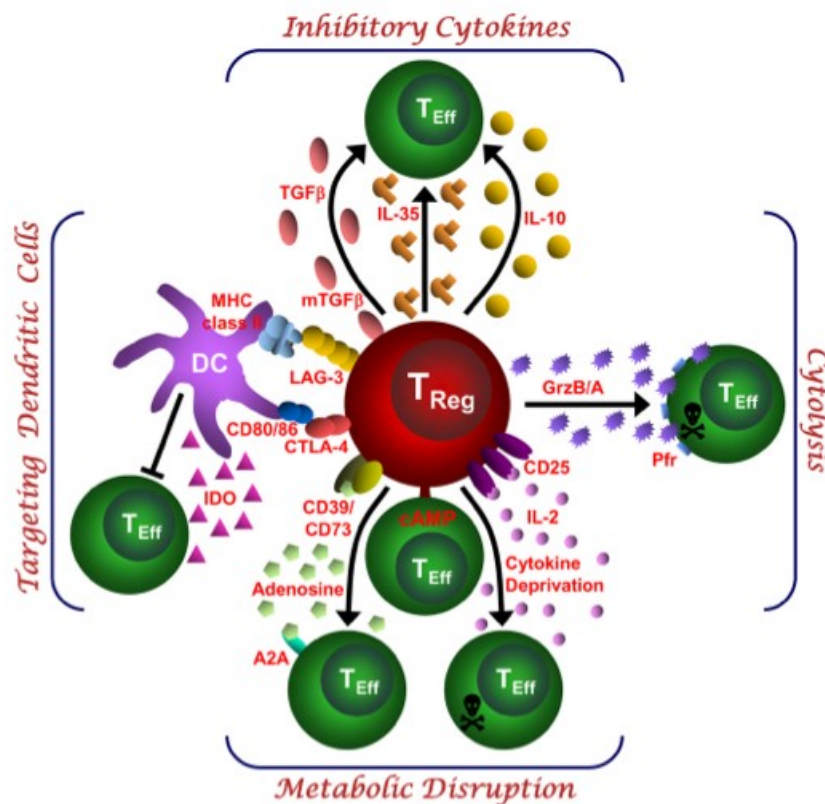


Figure 5: Four basic principles of T-cell suppression through Tregs (adapted from [15])

1.2.4 The Immune System in the CNS

The immune system of the central nervous system was traditionally described as an organ with „immune privilege“, stating that the immune reaction against antigens is less effective than in other tissues of the human body [16, 17]. The main reason is the unimpaired blood-brain-barrier that prevents the penetration of complement-factors, immunoglobulins and circulating inactivated immune cells into the brain. The strict description of the brain as an immunologically impaired organ was recently questioned with the identification of a slight number of T-cells in the healthy brain [18], a lymphatic drainage into the cervical lymph nodes [19] and an intrathecal expression of antibodies with an intact blood-brain-barrier [20]. Whereas the description of the CNS as a location of „immune privilege“ may apply within healthy

conditions, numerous diseases show humoral as well as cellular elements of the immune system in the CNS and liquor. Examples are cerebral infections, experimental autoimmune encephalitis (EAE), autoimmune diseases [21] and (within the case at hand) also brain tumors. Why primary brain tumors can exist in the CNS, whereas their metastases are mostly controlled by the immune system remains unclear. One can assume a potentiation of the previously described effects caused by the immunological conditions in the CNS as well as the escape-mechanisms of a tumor cell.

1.2.5 Tumor immunology in GBM

Although immune cells were found inside the GBM tumor site indicating an immune reaction of the host body against the tumor, the detailed mechanism and the reason for insufficiency in terms of tumor growth inhibition and elimination remain unclear. GBM seem to inhibit an anti-tumor immune response in the CNS by causing local and systemic immune-suppression through several hypothesized mechanisms [22].

Considerations include the fact that in specimen of GBM patients, tumor-infiltrating lymphocytes (TIL's) were identified. Among them the presence of immunosuppressive T regulatory cells (Treg) was seen [23]. Another cell type that might contribute to the immunosuppressive microenvironment of malignant gliomas are myeloid-derived suppressor cells (MDSCs). These cells comprise a heterogeneous population of myeloid cells that were shown to be significantly expanded in cancer patients and are associated with tumor progression.

1.3 Myeloid Derived Suppressor Cell's

1.3.1 Characteristics

In mice, MDSCs consist of a heterogeneous population of activated immature myeloid precursor cells that lead to immune suppression. They are known to accumulate in tissues of trauma patients, infectious disease, and septic conditions and were found to be present in bone marrow, liver, spleen, and tumor. In mice,

MDSCs were characterized through their marker profile of CD11b, CD33 and GR1, but the lack of the mature myeloid marker HLA-DR. The granulocytic marker GR1 includes both isoforms of Ly6C and Ly6G. Furthermore, a distinction in mice MDSCs was made between monocytic MDSCs (CD11b⁺Ly6G⁻Ly6C^{high}), and granulocytic MDSCs (CD11b⁺Ly6G⁺Ly6C^{low}) subtypes [24]. Both subtypes can suppress T cell function by the production of Arginase that decreases the level of L-arginine, which is critical for normal T cell function. Reduced levels of Arginine are known to reduce T cell receptor chain expression and to promote T cell dysfunction. MDSCs cells further have the property to secrete nitric oxide and reactive oxygen species, which are capable of inducing T cell suppression [25]. However tumor-free mice were found to contain the same phenotype of MDSCs in their peripheral blood system and lymphatic organs although in a much lower quantity. Tumor-associated MDSCs are believed to arise from immature myeloid progenitors through abnormal differentiation, which is promoted by factors in the tumor environment. Recruitment of MDSCs to the tumor site is regulated through cytokines and growth factors, such as granulocyte macrophage colony stimulating factor (GM-CSF), granulocyte colony-stimulating factor (G-CSF), interleukin (IL)-2, and vascular endothelial growth factor (VEGF) [26].

In humans, MDSCs were found in patients with solid and lymphatic tumor burden as well as in trauma and sepsis. The amount of isolated MDSCs in tumor patients was found to positively correlate with the tumor progression and metastasis. In contrast to MDSCs in mice, human MDSCs lack the GR1 marker and were therefore characterized by the monocyte/macrophage marker CD11b, the monocyte differentiation antigen CD14, the mature monocyte marker CD15, the myeloid lineage markers CD33, and the absence of HLA-DR, which is commonly expressed on myeloid cells. Therefore, a significant number of different phenotypes have been documented in tumors of different origins. Previously, it could be demonstrated that patients with newly diagnosed glioblastoma have an increased number of circulating CD33⁺ HLA-DR⁻ MDSCs in their blood that are composed of neutrophilic (CD15⁺), immature (CD15⁻CD14⁻), and monocytic (CD14⁺) subsets [27, 28]. Since none of the individual markers are unique to MDSCs, definitive identification of MDSCs was desired. MDSC antigens in humans and their known function that was used for the identification of human MDSC subsets in this thesis are listed below:

CD45 (PTPRC; Protein tyrosine phosphatase, receptor type c) is a single chain transmembrane receptor with intrinsic tyrosin phosphatase activity expressed exclusively on hematolymphoid cell membranes. It is counted to be an essential regulator of T and B cell antigen receptor-mediated activation. The disruption of its tyrosine kinase and phosphatase activity is a common trait in hematological malignancies[29].

CD14 is expressed mainly by macrophages, it acts as a co-receptor (along with the Toll-like receptor (TLR 4) and MD2) for the detection of bacterial lipopolysaccharide (LPS). Binding of antibody to CD14 does not trigger signal transduction since CD14 lacks a cytoplasmatic domain and therefore needs the presence of lipopolysaccharide-binding protein (LBP) to maintain its action.

CD15 (also called Lewis X) is a ligand for selectins and might be involved in cell adhesion through a direct CD15-CD15 interaction. CD15 is expressed mainly on mature granulocytes and monocytes but also on immature bone marrow cells [30]. CD15 mediates phagocytosis and chemotaxis, is found on neutrophils and plays a key role in the diagnosis of Hodgkin's disease as it is found on almost all Reed-Sternberg-cells.

CD11b (Integrin alpha M) is a protein that mediates inflammation by regulating leukocyte adhesion and migration it is involved in several immune processes such as phagocytosis, cell-mediated cytotoxicity, chemotaxis and cellular activation. CD11b is expressed on the surface of many leukocytes (monocytes, granulocytes, macrophages, and natural killer cells).

HLA-DR is an MHC class II cell surface receptor which presents (together with its intracellular digested ligand (antigen)) pathogens of foreign origin to the T-Cell receptors (TCR) on CD 4 / 8 T-cells, leading to their activation and differentiation into T-helper (CD4) and cytotoxic (CD8) T cells.

CD16 (FcyRIII) is expressed as a transmembrane protein on the surface of NK cells, activated monocytes and macrophages. CD16 binds aggregated IgG or IgG-antigen complex which functions in NK cell activation, phagocytosis, and antibody-dependent cell-mediated cytotoxicity (ADCC).

CD124 (IL-4R alpha chain) can bind and interact with IL-4 and consists of two types. The type I IL-4 receptor is present on T-, B-, NK, mast cells, basophils, and macrophages, whereas the type II IL-4 receptor is found mainly on non-hematopoietic cells and macrophages. IL-4 is responsible for the generation of IgE antibodies and for propagating the differentiation of naive Th0 cells into Th2 cells. In mucosal barriers, the IL-4 is involved in the recruitment of innate and adaptive immune effector cells.

1.3.2 Situation in different tumor entities

Oncological studies in humans have reported an increased frequency as well as immunosuppressive activity in some of the myeloid-derived subsets present in peripheral blood of patients with cancer [31, 32]. The accumulation of immature myeloid cells (IMCs) Lin (CD3/CD19/CD56/CD14/CD16) CD33⁺ HLA-DR^{-/low} in the blood correlates with the tumor burden as well as with the stage of the disease in two independent studies including a diverse set of cancer types [33]. Additionally, the frequency of either monocytic (CD11b⁺ CD14^{high} CD15^{positive}) or granulocytic (CD11b⁺ CD14^{low} CD15^{positive}) myeloid derived cells with immune-suppressive function have been found to be increased in patients with renal cell carcinoma [34], HCC [35], NSCLC [36], gastrointestinal [37], and prostate cancer [38]. Overviews of known oncological diseases with different MDSC subsets are displayed in Figure 6.

Subset	Disease type	Subset	Disease type
Lin ⁻ HLA-DR ⁻	HNSCC, lung, breast (N=93)	CD14 ⁺ HLA-DR ^{low/neg}	Multiple Myeloma (N=76)
Lin ⁻ HLA-DR ⁻ CD33 ⁺	Renal (N=18)	CD14 ⁺ HLA-DR ^{low/neg}	Melanom (N=16)
Lin ⁻ HLA-DR ⁻ CD33 ⁺	Melanoma (N=39)	CD14 ⁺ HLA-DR ^{low/neg}	Inflammatory Bowel disease (Ulcerative colitis: N=18; Crohn's disease: N=21)
Lin ^{-/low} HLA-DR ⁻ CD33 ⁺ CD11b ⁺	Renal (N=9)		HCC (N=111)
CD11b ⁺ CD14 ⁻ CD33 ⁺	Breast (N=17)	CD14 ⁺ HLA-DR ^{low/neg}	Melanoma (N=34)
CD33 ⁺ HLA-DR ⁻	HNSCC (N=14) and (N=5)	CD14 ⁺ HLA-DR ^{low/neg}	Prostate (N=40)
CD11b ⁺ CD14 ⁻ CD15 ⁺	Renal (N=23)	CD14 ⁺ HLA-DR ^{low/neg}	Renal (N=26)
CD11b ⁺ CD14 ⁻ CD15 ⁺	Renal (N=123)	CD14 ⁺	HNSCC (N=7)
CD11b ⁺ CD14 ⁻ CD15 ⁺ CD33 ⁺	Renal (N=27)		Multiple myeloma (N=7)
CD11b ⁺ CD33 ⁺	NSCLC (N=87)	CD14 ⁺ IL4Rα ⁺	Melanoma (N=14)
CD11b ⁺	Lung (N=10)		Colon (N=15)
CD15 ⁺ CD14 ⁻	Influenza A virus infection	CD15 ⁺ granulocytes	Pancreas (N=19)
CD15 ⁺ IL4Rα ⁺	Renal (N=23)		Colon (N=15)
	Melanoma (N=14)	SSC ^{high} CD66b ⁺	Breast (N=1)
	Colon (N=15)		HNSSC, lung, bladder and ureter (N=113)

Figure 6: Presence of myeloid derived suppressor cells in human diseases (adapted from [31])

2. Aim of this thesis

Myeloid-derived suppressor cells (MDSCs) are a heterogeneous population of myeloid cells that are significantly increased in cancer patients and are associated with tumor progression and poor overall survival. There is also a large body of evidence that the phenotype and function of MDSCs are largely dependent on the tumor type and specific conditions within the tumor microenvironment. MDSCs can suppress T-cell responses by several mechanisms including the depletion of specific amino acids such as L-arginine that are essential for T-cell function, and increased production of reactive oxygen species (ROS) (Figure 7). Furthermore, MDSCs suppression mechanisms include the ability of promoting de novo T-regulatory cell development. So far, the major difficulty in defining different human MDSC populations is that a specific marker is lacking.

The purpose of this thesis was to investigate the frequency and phenotype of MDSCs through a fluorescent activated cell sorter (FACS) as well as to investigate the function of myeloid-derived cells (MDSCs) in peripheral blood and freshly resected tumor samples in a cohort of 52 GBM patients. The aim was to characterise, analyse and correlate these findings with clinical presentation in the pursuit of a better understanding of the complex mechanisms involved in the tumor immunology of glioblastoma.

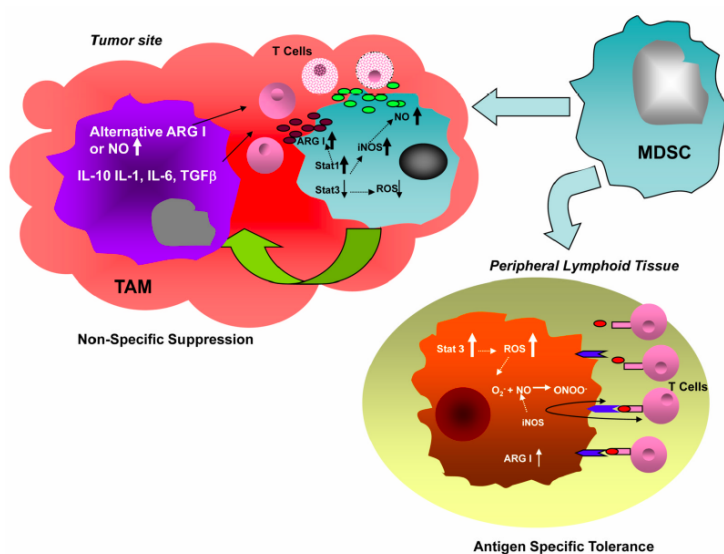


Figure7: Mechanisms of MDSC mediated immune suppression. (adapted from [39])

3. Material and Methods

3.1 Material

3.1.1 Disposable materials

Table2: Disposable materials

Material	Order number	Company
Cell Culture Flask 25cm ² (red cap)	83.1819.002	Sarstedt
6-well plate	83.392	Sarstedt
96-well plate	82.1581	Sarstedt
50 ml syringe	Original-Perfusor®	Braun
Butterfly needle	Sterican®	Braun
Petri dishes (145x20 mm sterile)	PP14	A.HartensteinLaborbedarf
Pipette Tips, white (10 µl)	T-300	Axygen, by Abimed
Pipette Tips, yellow (200 µl)	70.760.002	Sarsted
Pipette Tips, blue (1000 µ)	T-1000-B	Axygen, by Abimed
Scalpel	147222	Megro
Pasteur Pipettes	PP07	A.Hartenstein Laborbedarf
15 ml falcon tube	SS-3205	Sarsted
50 ml falcon tube	SS-7004	Sarsted

3.1.2 Chemicals and reagents

Table3: Chemicals and reagents

Material	Order number	Company
Lymphoprep 1,077g/cm ³	1114544	Axis-Shield
BiochromPBS Buffer (10x Dulbecco's)	A0965	AppliChem

DMSO	F-518	Finnzymes
EDTA	E5134	Sigma-Aldrich
Ethanol 99.8 %	9065.2	Carl-Roth
Glycerin Solution (for microscopy)	11513872	Leica
Glycerol	3783.1	Carl-Roth
Glycine	G7126	Sigma-Aldrich
Immersion Oil	11513859	Leica
Isopropanol	A0900	AppliChem
Paraformaldehyde	0335.1	Carl-Roth
PMA	P8139-1MG	Sigma-Aldrich
Ionomycin	I9657-1MG	Sigma-Aldrich

3.1.3 Kits

Table4: Kits

Kit	Order number	Company
Pan T-cell isolation kit	130-096-535	Miltenyi Biotec
Permeabilization Kit	88-8824-00	eBioscience

3.1.4 Media, reagents and supplements for cell culture

Table5: Media, reagents and supplements for cell culture

Media	Order number	Company
Dulbecco's Phosphate Buffered Saline	14190094	Invitrogen, Gibco
HBSS Ca ²⁺ /Mg ²⁺	14025050	Invitrogen, Gibco
Fetal Bovine Serum	SH30109.03	Thermo Scientific

RPMI	1640	Lifetechnologies
Fetal calf serum	26010074	Gibco, Invitrogen
Collagenase type IA	C0130	Sigma-Aldrich
DNase type I	D4527	Sigma-Aldrich
Trypsin-Inhibitor type I-S	T1021	Sigma-Aldrich
Propidiumiodide	P4170-10MG	Sigma-Aldrich
CFSE	21888-25MG-F	Sigma-Aldrich
DCFDA	D-399	Lifetechnologies
Brefeldin A	20350-15-6	Sigma-Aldrich
Penicillin-Streptomycin- Glutamine (100X)	10378-016	Thermo Scientific
1X permeabilization buffer	00-8333-56	eBioscience
Fixation/Permeabilization Diluent	00-5223-56	eBioscience

3.1.5 Antibodies

Table6: Antibodies

Antibodies	Order number	Company
CO-conjugated anti-CD45	17-9459	eBioscience
PE-Cy5.5–conjugated anti- CD14	11-1469	eBioscience
PB-conjugated anti-CD15	46-0158	eBioscience
PE-Cy5.5–conjugated antiCD11b	IM0530U	Beckman Coulter
Alexa-750–conjugated anti- CD16	56-0168	eBioscience
ECD-conjugated anti-HLADR	11-9952	eBioscience
PE-conjugated anti-CD124	14-1249	eBioscience

I-FITC anti-human Arginase	IC5868P	R&D Systems
FITC anti-sheep-IgG1	NL012	R&D Systems
APC-Alexafluor750 anti-CD3	A66329	Beckman Coulter
APC-Allophycocyanin anti-CD33	8017-0337	eBiosciences

3.1.6. Buffer

Table7: Buffer

Buffer	Annotation
Lyse-buffer	Ammoniumchlorid-solution (8,3g/l NH ₄ Cl, 1g/l KHCO ₃ , 0,0375g/l EDTA)

3.2 Methods

3.2.1 Patients characteristics

Tumor and blood specimens were collected from 52 patients with a median age 63.5 years (range 41 - 82). Blood samples were also collected from 26 age and gender matched healthy donors with a median age of 65,5 years (range 41-79) with no history of malignancies or autoimmune diseases and were enrolled in the study (Table 8). Written consent was obtained from all individuals before blood sampling and the ethical committee approved the study.

3.2.2 Intraoperative CUSA assisted resection of GBM

Glioma patients underwent 5-ALA assisted operation with general anesthesia, followed by craniotomy and tumor resection with the cavitron ultrasonic surgical aspirator (CUSA EXcel®). Tumor specimen were collected in the CUSA suction-bag that ultimately contained suspensions of single cells, tissue fragments, and blood in saline. The CUSA apparatus is used as a routine device in resections of brain tumors since its introduction by Flamm [40]. Compared with the small diagnostic-biopsy samples of brain tumors, ultrasonic surgical aspirations contain generous amounts of

tumor cells in large volumes of fluid. Through a computerized control unit, with settings for different amplitudes of ultrasonic waves and speeds of irrigation and aspiration, the ultrasonic apparatus is an efficient intraoperative device for brain tumor resection. Tumor tissues are targeted and selectively aspirated. An advantage of the ultrasonic aspiration technique over surgical tissue dissection is the reduced need for retraction of normal brain-tissue and a decreased injury of neurons and glia cells in the patient's brain. The aspirated content was evacuated into a sterile pouch and sent to the laboratory, where the aspirated material was processed immediately (Figure 8).



Figure 8: left: intraoperative view of Glioblastoma resection situs with the CUSA apparatus, right: laboratory setting before proceeding the specimen

3.2.3 Isolation of tumor infiltrated leucocytes (TIL's) from tumortissue

Ultrasonic aspirates were collected in a closed system disposable suction bag. Tumor fragments were washed extensively with PBS to discard blood and suction fluid. Tumor fragments were cut into small pieces and incubated with Collagenase type IA (100 mg/mL), DNase type I (10 µg/mL) and a trypsin inhibitor type I-S from Glycine max in HBSS with Ca²⁺ and Mg²⁺ at 37°C. After 45 minutes, EDTA was added (12.5 mM final), the cell suspension prepared, filtered and transferred into a 15 ml falcon tube. After sedimentation at 1g for 30 min, the supernatant was collected and loaded on a modified Ficoll gradient (75% Ficoll/25%RMPI supplement with 10% FCS). The interphase containing mainly myelin debris and dead cells was removed, and the pellet was immediately used for further analysis after washing.

3.2.4 Isolation of peripheral blood mononuclear cell's (PBMC) from venous blood

After a detailed medical clarification, the blood sample was withdrawn from a periphery vein. For isolation of the mononuclear cells, the density gradient centrifugation method was used. The venous blood was carefully underlayered with 15ml Lymphoprep. After centrifugation with 740g without break at 20 °C for 20 minutes, the mononuclear cells became visible in a solid layer between the Lymphoprep and the plasma supernatant, and could be rescued with a manual pipet and transferred into a 50ml falcon tube. In the following washing step the mononuclear cell containing falcon tube was filled up with cold PBS and again centrifuged at 500 g for 7 minutes at 4 °C. 25ml Lyse-buffer was added and resuspended with the gained cell sediment, thereafter incubated for 10 to 15 minutes on a shaking platform at 4 °C in order to lyse the remaining erythrocytes. Accordingly, the previously described washing step was repeated twice, and the cell sediment was thereafter resuspended in FCS and immediately used for further proceedings or conserved at 4°C over night.

3.2.5 Fluorescent activated cell sorting (FACS)

To determine the frequency and phenotype of MDSCs in freshly isolated PBMCs and tumor cell suspensions they were stained for 30 min at 4°C using a panel of directly labeled monoclonal antibodies (mAbs): CD124-PE (Phycoerythrin), HLADR-ECD (Phycoerythrin-Texas Red-X), CD14-PC5.5 (Phycoerythrin-Cyanin 5.5), CD11b-PC7 (Phycoerythrin-Cyanin7), CD33-APC (Allophycocyanin), CD16-APC-Alexafluor750, CD15-PacificBlue, PE-Cy5-conjugated anti-CD3 and CD45-KromeOrange . Viability of CD45⁺ cells was checked by propidiumiodide and it usually was >95%. After washing, all samples were analyzed using the NaviosTM flow cytometer and the Kaluza 1.2 Software (Beckman Coulter, Germany).

3.2.6 Cytospin preparation

A labeled slide, chamber and blotter for each sample was prepared and cells resuspended in HBSS containing 30% FCS to a concentration of approximately 5×10^5 cells/ml. Next 200 μ l of each cell suspension was added to a slide chamber and a spindown at 800 rpm for 5 minutes was performed. The slide was carefully removed from the cytocentrifuge and cells were allowed to air dry prior to staining.

3.2.7 ROS detection

Oxidation-sensitive dye, dichlorodihydrofluorescein diacetate (DCFDA), was used to measure ROS production by MDSC. Cells were labeled with 1 μ M DCFDA for 10 minutes at 37 °C in PBS 1% FCS, washed twice and then incubated in complete medium (IMDM with L-glutamine containing 10% fetal calf serum, antibiotics (penicillin 100 U/mL, streptomycin 100 mg/mL)) for 30 minutes at 37°C. DCFDA-labeled cells were then stained with MDSC surface antibodies as described above. After 30min incubation on ice, cells were washed twice with cold PBS and analyzed by color flow cytometry. Aliquots of Ab-stained cells which were not incubated with DCFDA served as controls.

3.2.8 Arginase detection

For intracellular Arginase I staining, the eBioscience Fixation/Permeabilization procedure was used. TILs and PBMCs obtained from GBM patients were washed and fixed by adding 100 μ L of IC Fixation Buffer and pulse vortexing the cocktail. Next cells were incubated under dark conditions at RT for 40 minutes. 2mL of 1X permeabilization buffer was added and centrifugation of the samples at 400g for 5 minutes was performed. The supernatant was discarded and the previous step repeated. The cells were resuspended in 100 μ L of 1X Permeabilization Buffer and the I-FITC antibody was added and incubation for 40 minutes under dark condition at RT was performed. 2mL of 1X Permeabilization Buffer, added to the solution and the sample was centrifuged at 400g for 5 minutes under RT. The supernatant was discarded and 2mL of flow cytometry staining buffer was added. The washing step was repeated and the cells were resuspended in 5mL flow cytometry staining buffer

and analysed with the flow cytometer. Sheep IgG control Ab was used as negative control.

3.2.9 MRI scans and tumor volume measurement

All MRI examinations were performed with a 1.5-T clinical imaging system (Gyroscan Intera®; Philips Medical Systems, Best, The Netherlands) using a synergy head/neck coil. For volumetry contrast-enhanced axial and coronal or sagittal T1-weighted sequences were used. Tumor volume was calculated by the ellipsoid formula $(4 \times \pi \times d1/2 \times d2/2 \times d3/2)/3$ using the largest diameters in the axial plane and the largest diameter in the orthogonal plane.

3.2.10 T-cell proliferation assay

For T-cell proliferation assay, T cells were purified using a Pan T-cell isolation kit. Cells were resuspended in 40 μ L of buffer and 10 μ L of Pan T Cell Biotin-Antibody Cocktail was added. After vortexing cells were incubated for 5 minutes in the refrigerator at 6°C. Next 30 μ L of buffer and 20 μ L of Pan T Cell MicroBead Cocktail was mixed together and incubated for 10 more minutes at 6°C. Staining antibody anti-CD3 (10 μ g/ml) was added and 5 more minutes of incubation under dark condition was performed. For magnetic separation MACS Column and MACS Separator were assembled according to manufacturers manual. The column was prepared by rinsing 3L of buffer. The cell suspension was applied onto the column and the unlabelled flow through representing the T-Cells enriched fraction was collected into a 5mL tube. T-cells were next labeled with 1 μ M CFSE for 5 minutes in PBS containing 1% FCS, washed twice and seeded in a 96-well round-bottom plate coated with coated human anti-CD3 mAbs (10 μ g/ml) at 5×10^4 /well and were cocultured with MDSC-enriched subset cell ratios of 1/1 and 2/1 or 4/1 for 5 days at 37°C in complete medium in the presence of 100 U/ml IL-2. T-cell proliferation was monitored by FACS analysis of CFSE fluorescence intensity after staining with PE-Cy5-conjugated anti-CD3 mAbs. T-cells in culture medium alone were used as

background controls. Cocultures were conducted in triplicates. After 5 days, cells were harvested, stained with anti-CD3-PC5.5 and were analyzed by FACS.

3.2.11 Intracellular INF- γ detection

For intracellular IFN- γ detection, PBMC, TILs or CFSE-labeled T-cells were stimulated with phorbol 12-myristate 13-acetate (PMA, Sigma-Aldrich, Germany; 100 ng/mL) plus ionomycin (Sigma-Aldrich, Germany; 1 μ g/mL) overnight (16 hours) in the presence of Brefeldin A (10 μ g/ml). Cells were then stained with T-cell markers, further processed with the Fixation/Permabilization Kit from eBioscience, and labeled with a PE-conjugated IFN- γ mAb (Beckman Coulter, Germany).

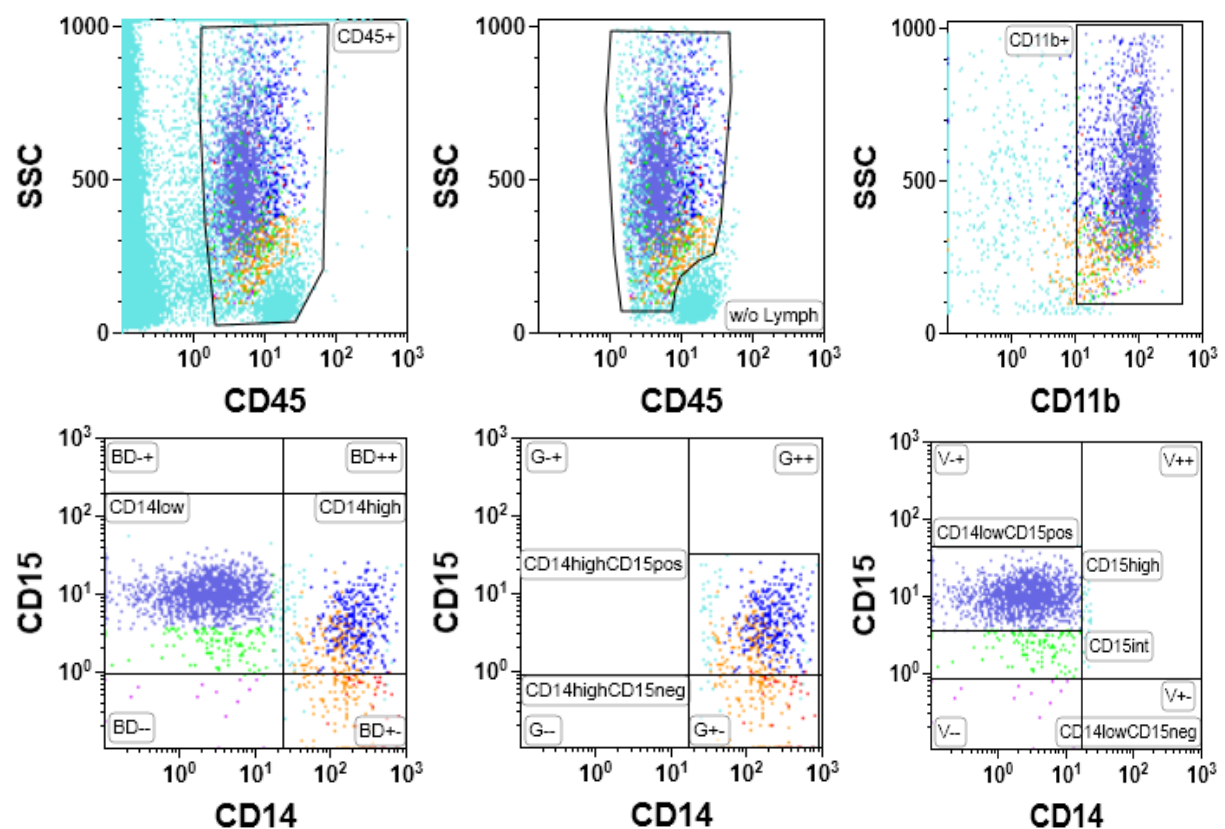
3.2.12 Statistic

The data were analyzed with the Kolmogorov–Smirnov procedure to test for normal distribution. Since not all groups showed a normal distribution, the following non-parametric tests were used: The two-tailed Mann-Whitney test was used to test for significant differences between two groups. The Kruskal–Wallis test with post hoc Dunn Multiple Comparison analysis was applied to test for significant differences between three and more groups. For correlation analysis, we used the Spearman rank test. Values of $p < 0.05$ were considered to be significant. Error bars represent the SE of the mean. GraphPad Prism 5.0 (GraphPad Software Inc., USA) was used for statistical analyses.

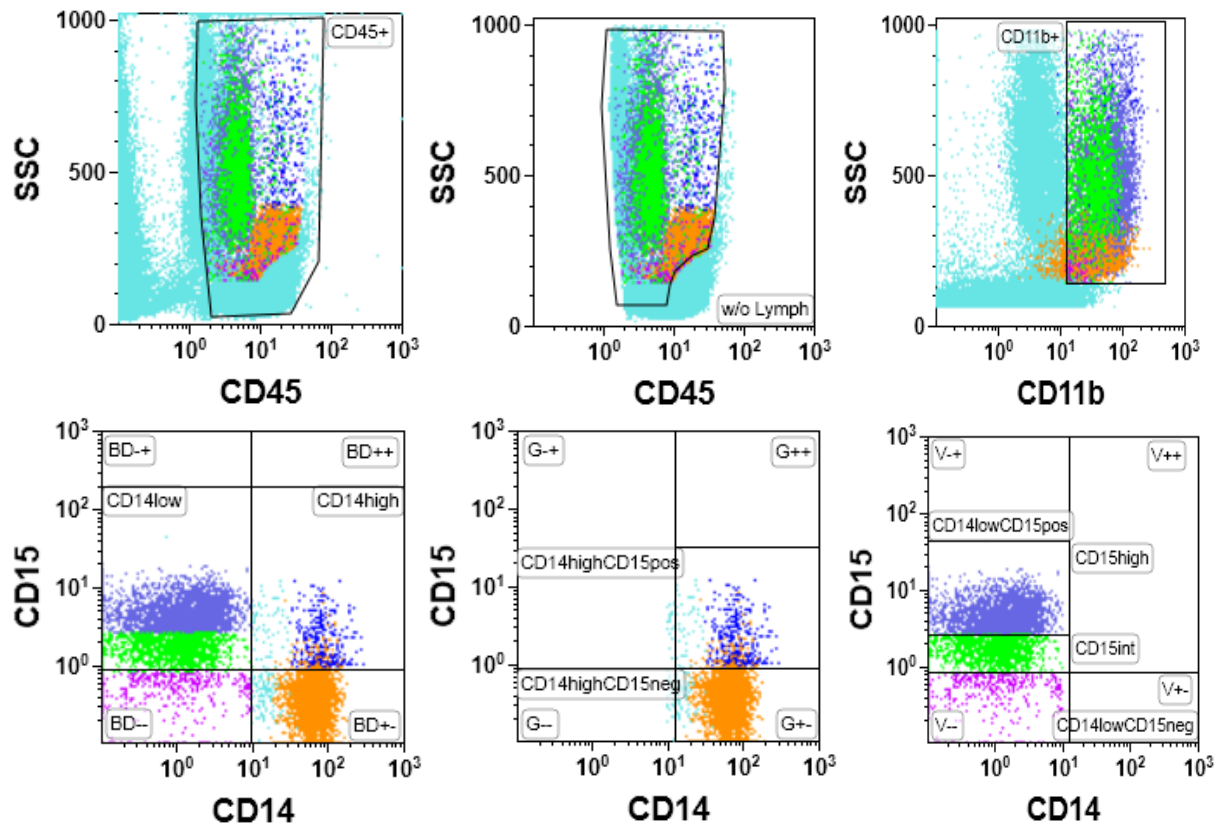
4.Results

4.1 Phenotype, morphology and frequency of different MDSC subsets in peripheral blood and tumor tissue of primary glioblastoma patients

In order to analyze the different subsets of MDSCs in the peripheral blood and tumor tissue of primary glioblastoma patients, PBMCs obtained from the periphery blood and TILs obtained from the tumor specimen were enzymatically digested as described in the material and method section. MDSCs were gated from TIL and PBMC according to their CD45 antibody binding and CD11b positivity was further gated through PC7 antibody binding. CD11b^{positive} as well as CD45^{positive} cells were then further gated according to their CD14 and CD15 marker expression. The gating strategy is shown in Figure 9. Cells expressing a low amount of CD14 were further split into CD15^{high}, CD15^{negative} and CD15^{intermediate} subgroups. Cells showing a high CD14 expression were further subdivided into CD15^{high}, CD15^{intermediate} or CD15^{negative}.



A



B

Figure9: Gating strategy for the assessment of the MDSC population from tumor infiltrating leucocytes and periphery blood mononuclear cells, using flow cytometry in GBM patients. A: Cells obtained from tumor tissue. B: Cells obtained from peripheral blood

4.2. Patients characteristic n=52

Table8: Patients characteristic n=52

Number of patients		52 (100%)
Sex		
	male	33 (63%)
	female	19 (37%)
Median age	years	63,5 (41-82)

Resection status		
	complete	25 (48%)
	incomplete	27 (52%)
Mean tumor volume		
	pre-surgery	42,2 cm ³
Steroids		
	received	34 (65%)
	not received	18 (35%)
MGMT status		
	methylated	17 (33%)
	unmethylated	35 (67%)

4.3 Morphologic characteristics of different MDSCs subsets

For morphological analysis, cytopins were performed and cells were stained with hematoxylin and eosin. Representative pictures of the MDSC subsets are shown in Figure 10. CD14^{high}CD15^{positive} cells displayed typical features of monocytes with a lobulated or reniform nucleus usually eccentrically placed, and a grayish-blue cytoplasm. CD14^{low}CD15^{high} cells revealed the typical morphology of neutrophils with segmented nuclei and pale pink cytoplasm. CD14^{low}CD15^{intermediate} cells displayed features of eosinophils with a classic bilobed nucleus and eosinophilic cytoplasm filled with numerous red granules of uniform size. CD14^{low}CD15^{negative} showed big round nuclei with a small basophilic cytoplasm characteristic for immature myeloid cells.

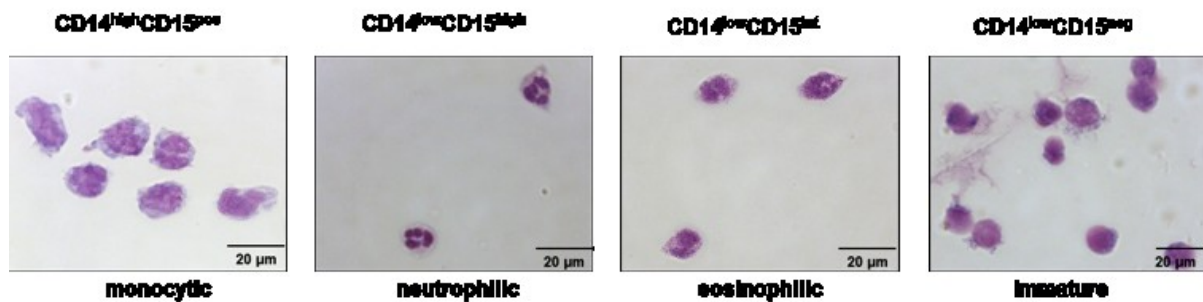


Figure 10: Morphologic characteristics of different MDSC subsets in the peripheral blood of glioblastoma patients. Myeloid cells were labeled with anti-CD11b and anti-CD14 antibodies and after sorting four major MDSC subpopulations were defined: $CD14^{high}CD15^{positive}$ are further referred to as a monocytic phenotype, $CD14^{low}CD15^{low}$ MDSCs showed characteristics of immature myeloid cells and the $CD14^{low}CD15^{positive}$ granulocytic phenotype consisted of $CD14^{low}CD15^{high}$ neutrophils and $CD14^{low}CD15^{intermediate}$ eosinophils

The flow cytometry evaluation of the different subsets of peripheral blood mononuclear cells and their expression intensity of CD14 and CD15 from blood obtained from patients with Glioblastoma is shown in Figure 11. GBM patients had an increased percentage of monocytic $CD14^{high}CD15^{positive}$ MDSCs and neutrophilic $CD14^{low}CD15^{high}$ MDSCs in their peripheral blood when compared to healthy donors, whereas the percentage of immature $CD14^{low}CD15^{negative}$ MDSCs was significantly reduced. Moreover, a significant increase in the frequency of both monocytic $CD14^{high}CD15^{positive}$ and neutrophilic $CD14^{low}CD15^{positive}$ MDSCs at the tumor site could be shown.

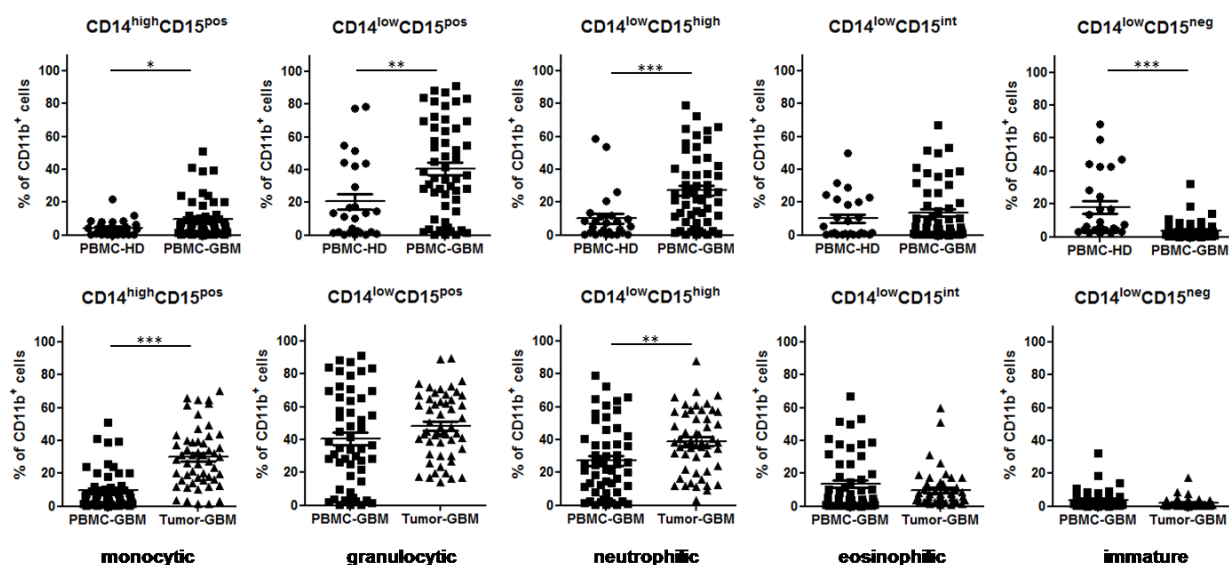


Figure 11: shows different subtype distributions of MDSCs in GBM patients. Healthy donors N=26, GBM N=52.

4.4 Distribution of different MDSCs subsets within PBMC and TILs of healthy donors (HD) and glioblastoma patients (GBM)

Table9: Distribution of different MDSCs subsets within PBMC and TILs of healthy donors (HD) and glioblastoma patients (GBM)

Population	PBMC- HD	PBMC- GBM	P- value	PBMC- GBM	TIL- GBM	P-value
	%	%		%	%	
CD11b ^{high} %CD45 (w/o Lymph)						
Mean	53,21	56,62	0.5264	56,62	25,31	<0.0001
Std. Deviation	25,92	20,44		20,44	14,88	
CD14 ^{high} CD15 ^{pos}						
Mean	3,420	9,668	0.0018	9,668	29,95	<0.0001
Std. Deviation	4,464	11,95		11,95	18,24	
CD14 ^{low} CD15 ^{pos}						
Mean	28,32	40,56	0.0339	40,56	48,47	0.1226
Std. Deviation	24,75	28,65		28,65	19,84	
CD14 ^{low} CD15 ^{high}						
Mean	13,61	27,06	0.0020	27,06	38,76	0.0029
Std. Deviation	14,73	21,97		21,97	18,86	
CD14 ^{low} CD15 ^{int}						
Mean	14,24	13,57	0.3930	13,57	9,753	0.4372
Std. Deviation	13,08	17,39		17,39	11,35	

CD14 ^{low} CD15 ^{neg}						
Mean	22,71	3,891	<0.000 1	3,891	2,223	0.0980
Std. Deviation	19,22	5,425		5,425	2,715	

4.5 Phenotypic analysis of MDSC subpopulation in peripheral blood and tumor

To further investigate the phenotype of MDSC according to their expression profile, all four previously described MDSC subgroups were stained with HLA-DR, CD16 and CD124 antibodies as listed in the material and methods section.

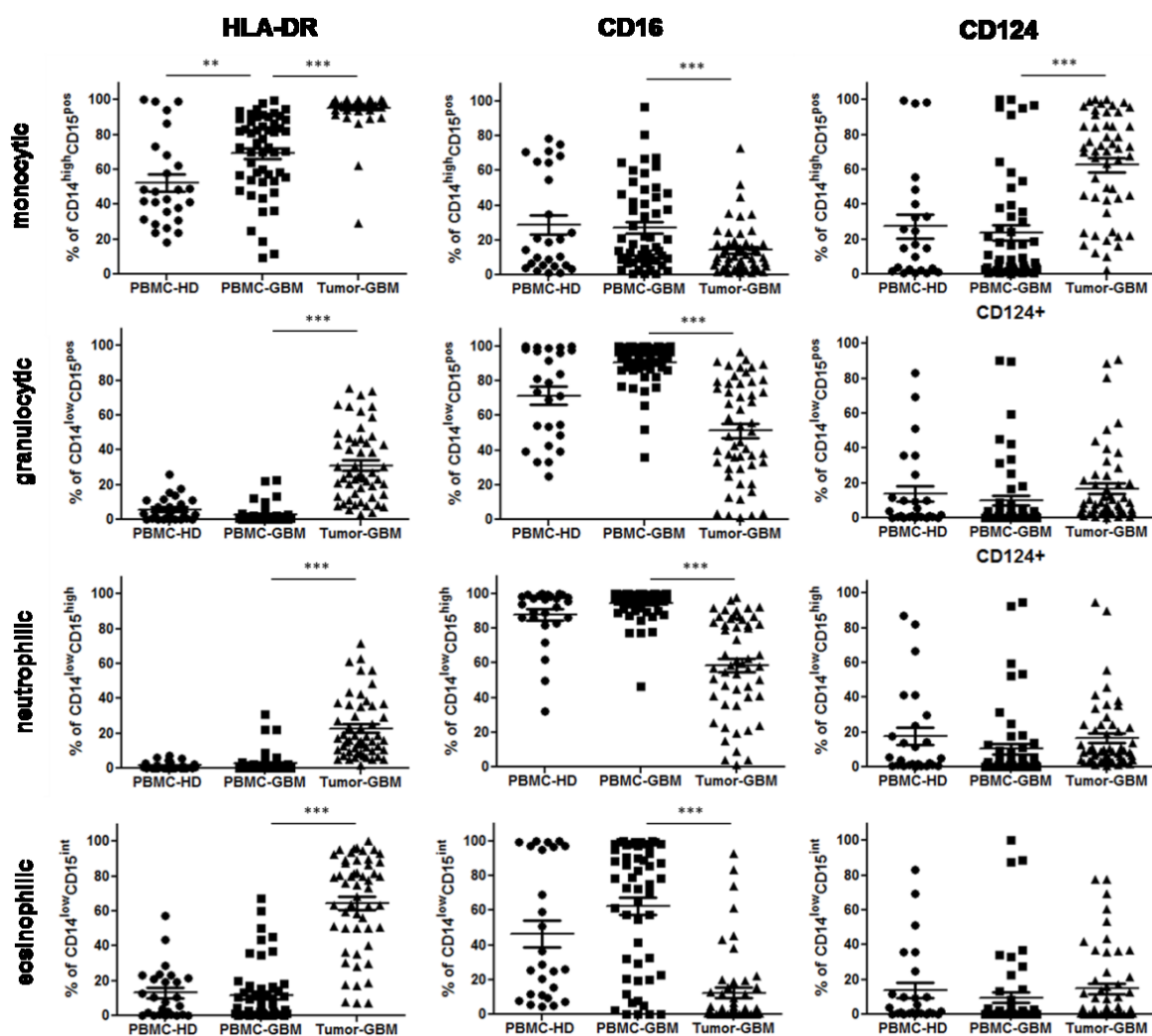


Figure12: Phenotypic analysis of monocytic, granulocytic, neutrophilic and eosinophilic MDSCs in peripheral blood (PBMC), tumor specimen (TIL) and healthy donors (HD)

Figure 12 demonstrates that HLA-DR was significantly upregulated on the monocytic phenotype MDSCs from peripheral blood of glioblastoma patients when compared to healthy donors, whereas the granulocytic phenotype MDSCs remained negative for HLA-DR. In contrast, HLA-DR was significantly upregulated on both tumor-infiltrating monocytic and granulocytic MDSCs, mainly on the eosinophilic MDSCs subtype.

Moreover, a significant down-regulation of CD16 on tumor-infiltrating monocytic and granulocytic MDSCs could be shown, when compared to MDSCs in the peripheral blood of glioblastoma patients. Remarkably, up-regulation of CD124 (IL4R α chain) was mainly restricted to tumor-infiltrating monocytic MDSCs.

4.6 Influence of steroid ingestion and MGMT status on MDSCs subgroups

Steroids are known immunosuppressants and are widely used therapeutically. In terms of GBM the surrounding edema is usually responsible for the onset of neurological symptoms. The initial application of steroids improves the edema through a stabilisation of the blood brain barrier, but has no curative benefit. The influence of steroid ingestion on the presence of the different MDSCs subsets in the periphery cells as well as in the tumor was further investigated. Figure 13 shows the distribution of MDSCs comparing patients who received steroids (n=34) vs patients without steroid use (n=18). Interestingly the ingestion of steroids showed no significant difference for cells obtained from peripheral blood or tumor.

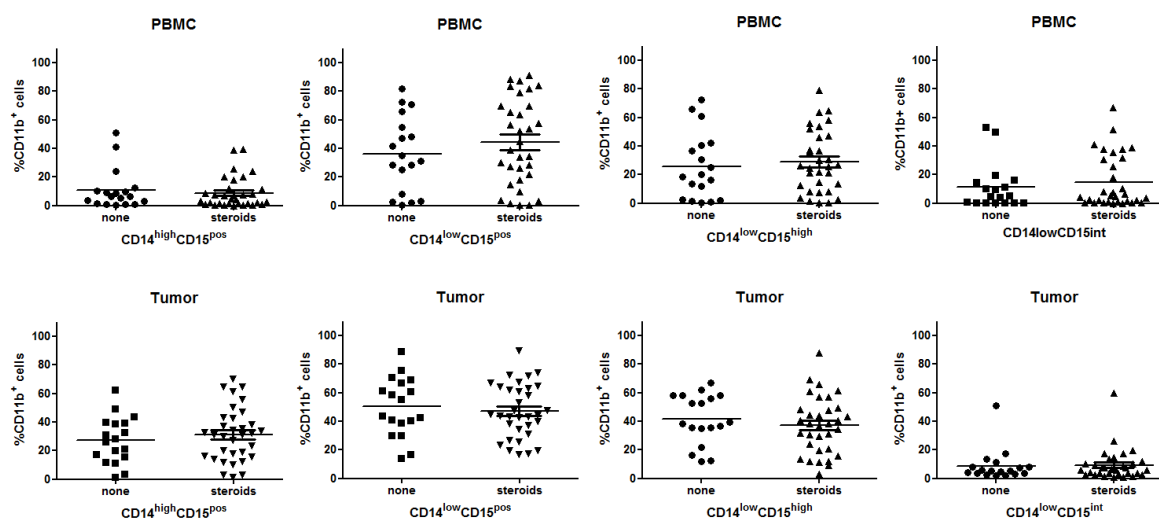


Figure13: MDSC distribution in the tumor and peripheral blood with and without steroid ingestion

As previously described in the introduction, the MGMT promoter methylation status is an important marker in terms of chemotherapy response and overall survival. Therefore, the correlation between MGMT methylation status of the tumor and MDSC distribution in the tumor and peripheral blood was investigated. As displayed in Figure 14, we could not detect significant differences in the frequency of MDSC subsets in peripheral blood and tumors between MGMT methylated or unmethylated tumors.

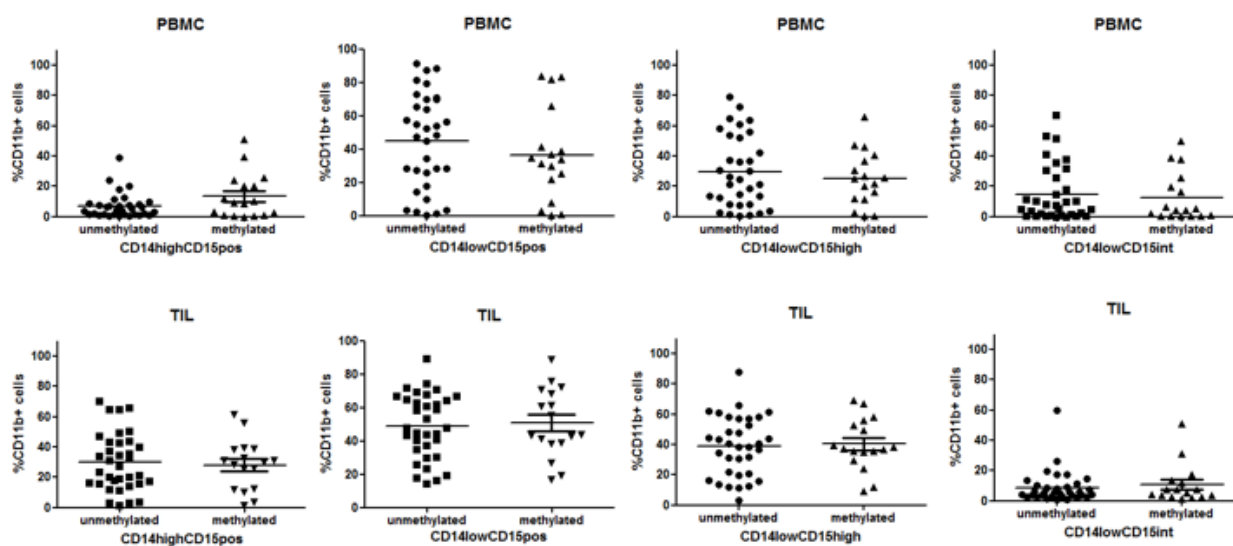


Figure 14: MDSC distribution in the tumor and peripheral blood according to MGMT promoter methylation status .

4.7. DCFA and ARG1 expression of MDSC subpopulation in PBMCs and TILs in GBM

We could demonstrate that MDSCs in patients with glioblastoma show a different expression profile of cell surface markers. Next, we examined the activation status of these cells. For our analysis, a general oxidative stress indicator dye DCFDA was used. This fluorescent dye measures hydroxyl, peroxy and other reactive species (ROS) activity within the cell. After diffusion into the cell, DCFDA is deacetylated by cellular esterases to a non-fluorescent compound, which is later oxidized by ROS into DCF. DCF is highly fluorescent and can be detected with fluorescent spectroscopy at a maximum emission of 495nm. After staining the four subgroups of tumor and peripheral blood MDSCs according to the procedure described in the material and methods section the fluorescent analysis was performed and the result is shown in Figure 15. As displayed, all four subtypes of MDSCs produced ROS in both MDSC subsets, but mainly in peripheral blood.

Next, Arginase 1 expression of MDSCs was investigated. Arginin is essential for cytotoxic immune reaction of CTL cells and one of the proposed immunosuppressive mechanisms of MDSCs. It is hypothesised that MDSCs secrete Arginase, which degrades the amino acid Arginin. To study the role of TILs and PBMCs among MDSC in GBM patients Arginase 1 expression was studied with the Fixation/Permeabilization method described in the material and methods section. The intracellular staining for Arginase 1 is shown in Figure 15. Arginase 1 was strongly upregulated in tumor-infiltrating MDSCs, predominantly in monocytic MDSCs, whereas only a minor fraction of MDSCs in peripheral blood expressed Arginase 1. This data demonstrates different intracellular up regulations of Arginase1 between MDSCs obtained from PBMCs and TILs.

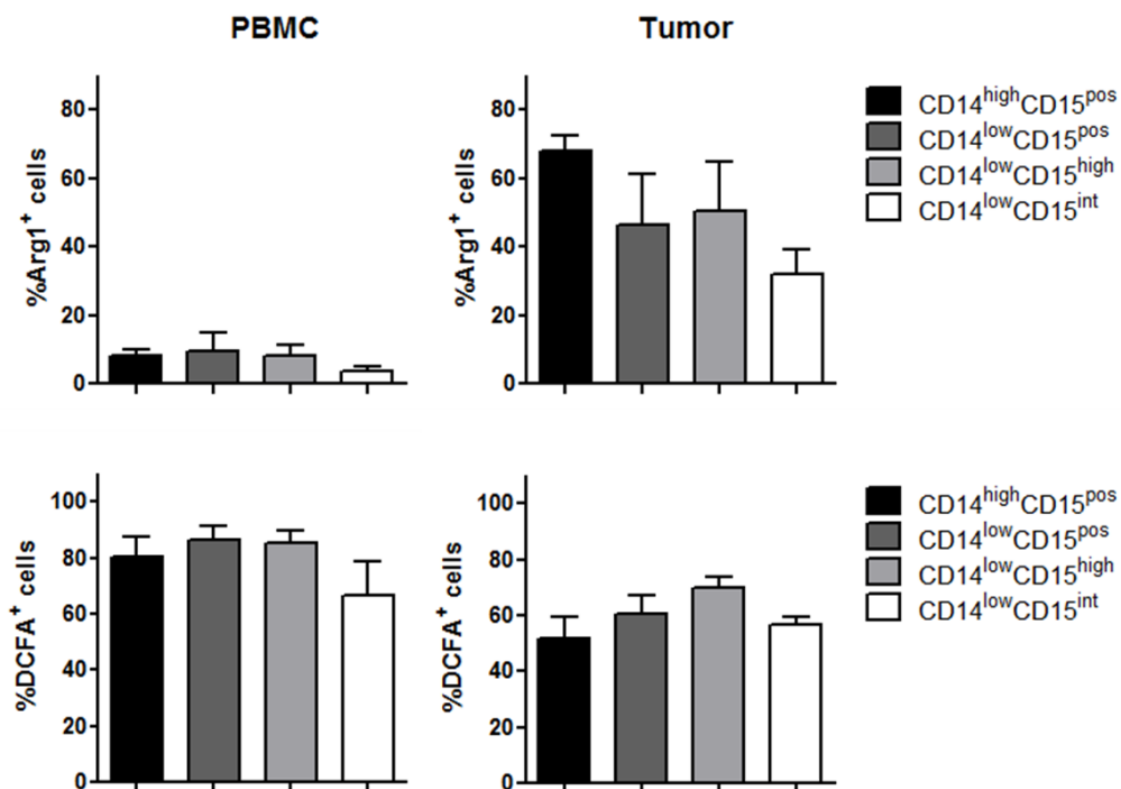


Figure15: Arginase 1 (Arg1+) and ROS (DCFA+) expression of the four different subtypes obtained from peripheral blood and tumor

4.8 T-Cell suppression assay of sorted MDSC subpopulations

As MDSC seems to modulate the immunologic response of GBM patients, the next question was whether MDSCs suppress T-cell responses. Therefore, freshly prepared MDSCs from peripheral blood and tumor material of the same patient were sorted by flow cytometry and analyzed in an autologous non-specific T-cell proliferation assay. After co-cultivation of T-cells and MDSCs at a 2:1 ratio for 5 days, T-cells were harvested and labeled with the fluorescent dye CFSE. CFSE binds to any cellular protein with primary amines and during cell division the dye is distributed equally between daughter cells. This can be measured as successive halving of the fluorescence intensity of the dye. For FACS analysis of T-cells the anti-CD3 antibody was used. As shown in Figure 16, granulocytic, and mainly neutrophilic blood-derived MDSCs significantly reduced T-cell proliferation, whereas tumor-derived MDSCs did not suppress T-cell proliferation *in vitro*. The same pattern could be observed with $CD14^{high}CD15^{positive}$ cells of monocytic phenotype. Representative dot plots of T cell proliferation and intracellular INF- γ secretion after addition of $CD14^{low}CD15^{high}$ neutrophilic MDSCs to CFSE-labeled autologous T-cells at different T-cell: MDSCs ratios (1:1 – 4:1) and PMA/ionomycin stimulation is shown in Figure 17. The percentage values represent the fraction of INF- γ secreting CFSE-labeled T-cells.

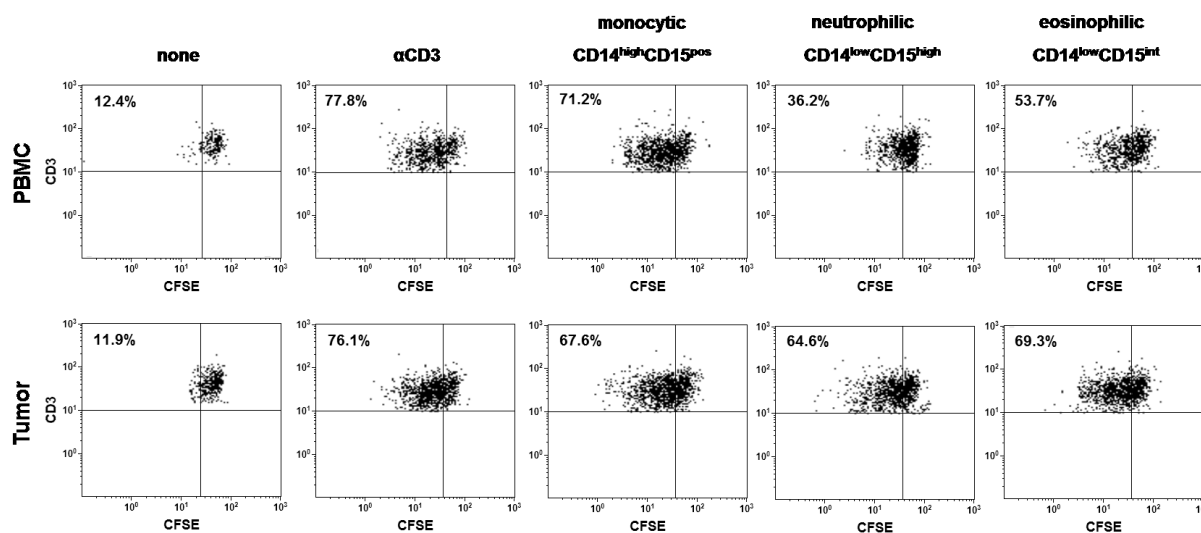


Figure16: T-cell suppression assay with autologous CFSE-labeled T-cells and FACS-sorted MDSC subsets obtained from PBMC or tumor suspensions at a ratio of 2:1.

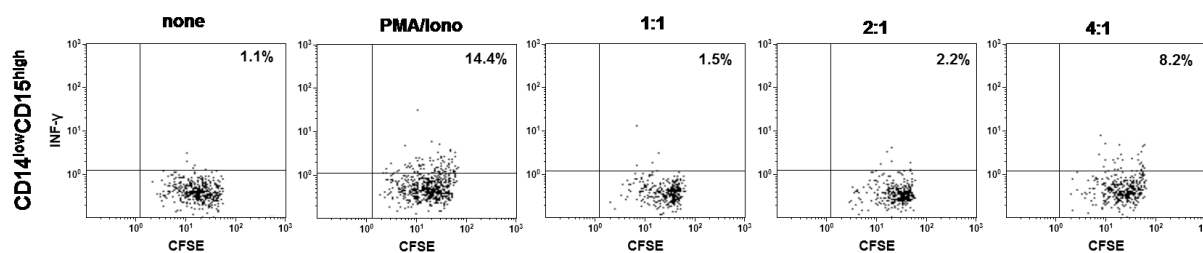


Figure17: Representative dot plots of T cell proliferation and intracellular INF- γ secretion after addition of neutrophilic MDSCs to CFSE-labeled autologous T-cells and PMA/ionomycin stimulation

4.9. Frequency of MDSCs in the tumor is dependent on the pre-operative tumor volume

To gain a deeper insight into the dynamics of MDSC attraction to the tumor site, correlations between the frequency of MDSC subsets in the tumor tissue and the tumor volume before resection was investigated. Therefore, the pre-operative tumor volume on MRI was calculated as described in the material and methods section and correlated to the proportion of MDSC subsets within the tissue obtained from tumor resection. Regression analysis showed that the frequency of granulocytic ($p=0,0006$), neutrophilic ($p=0,0172$) and eosinophilic ($p=0,0066$) MDSCs positively correlated with the tumor volume before resection, whereas a negative association between the frequency of monocytic ($p=0,0060$) and the tumor volume before resection was found (Figure 18). For MDSCs obtained from peripheral blood no correlation between pre- and postoperative analysis could be found (data not shown).

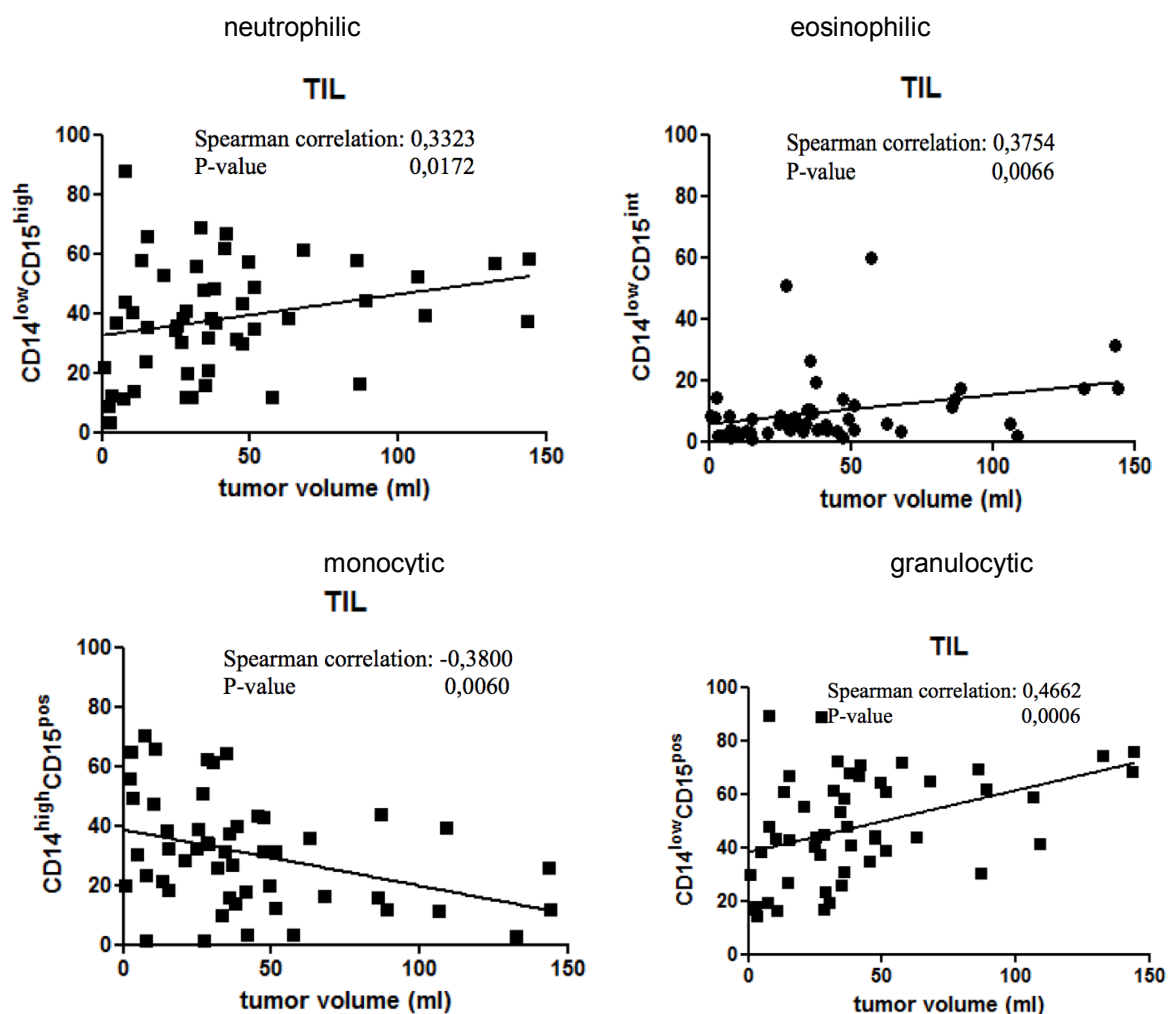


Figure18: Correlation between the proportion of granulocytic, neutrophilic, eosinophilic and monocytic MDSCs within TILs (n=52) and the tumor volume before tumor resection

4.10 Correlation of MDSCs with Tregs in peripheral blood and tumor and time to tumor progression

The mechanism by which Tregs limit anti-tumor immunity is not fully understood to date. Therefore, the correlation of Tregs and granulocytic or monocytic TIL and PBMC subtypes of MDSCs was investigated next. As depicted in Figure 19, significant correlation between these MDSC subsets and tumor-infiltrating CD4⁺ T-cell regulatory T-cells could not be found.

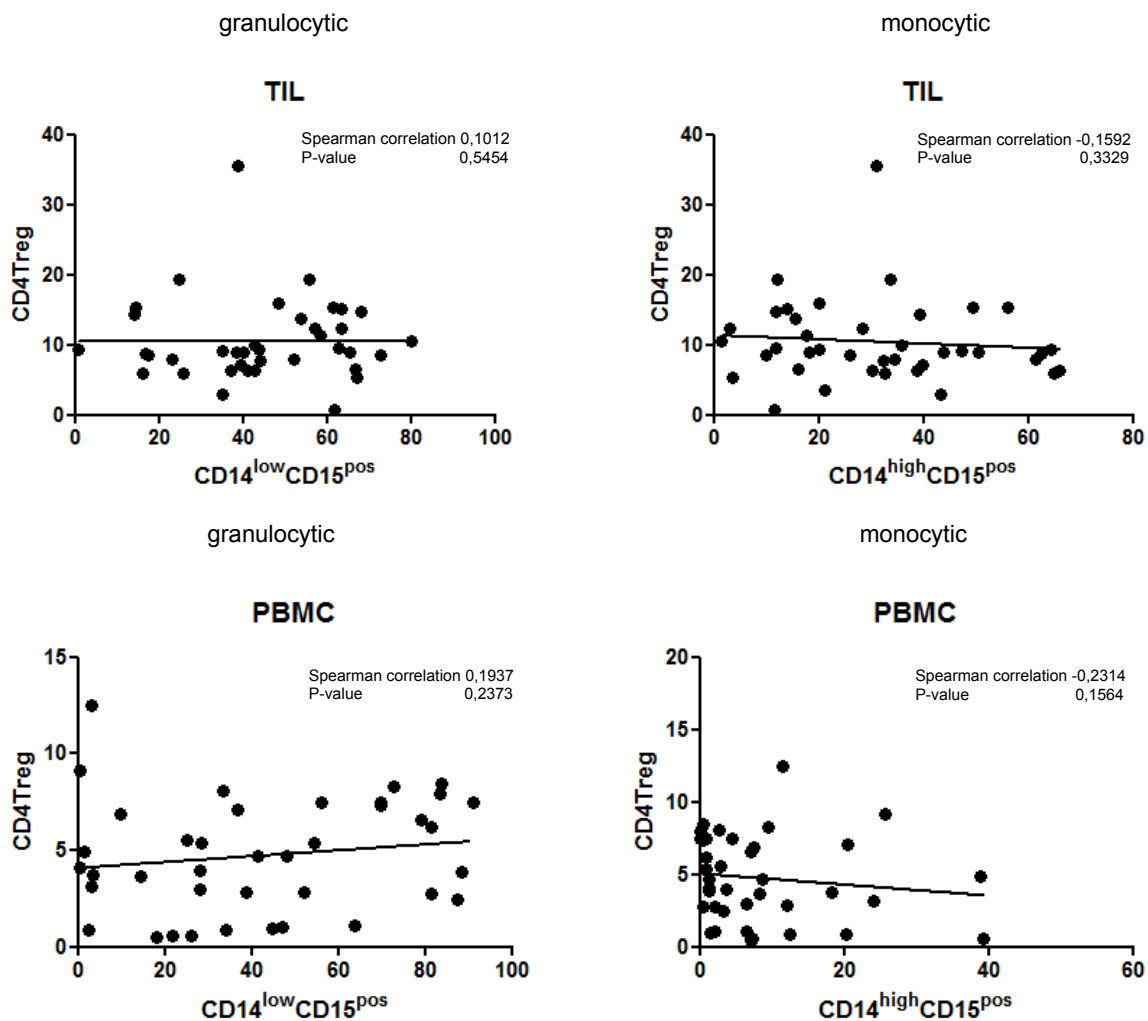


Figure19:Correlation between the proportion of granuloctytic and monocytic TIL and PBMC MDSCsand CD4 Treg (n=39).

Next, the correlation between the presence of granuloctytic and monocytic MDSCs and time to tumor progression was investigated (follow-up were only available for 28 patients). Summarising, no relevant correlation between these MDSC subsets and time to progression was observed (Figure 20).

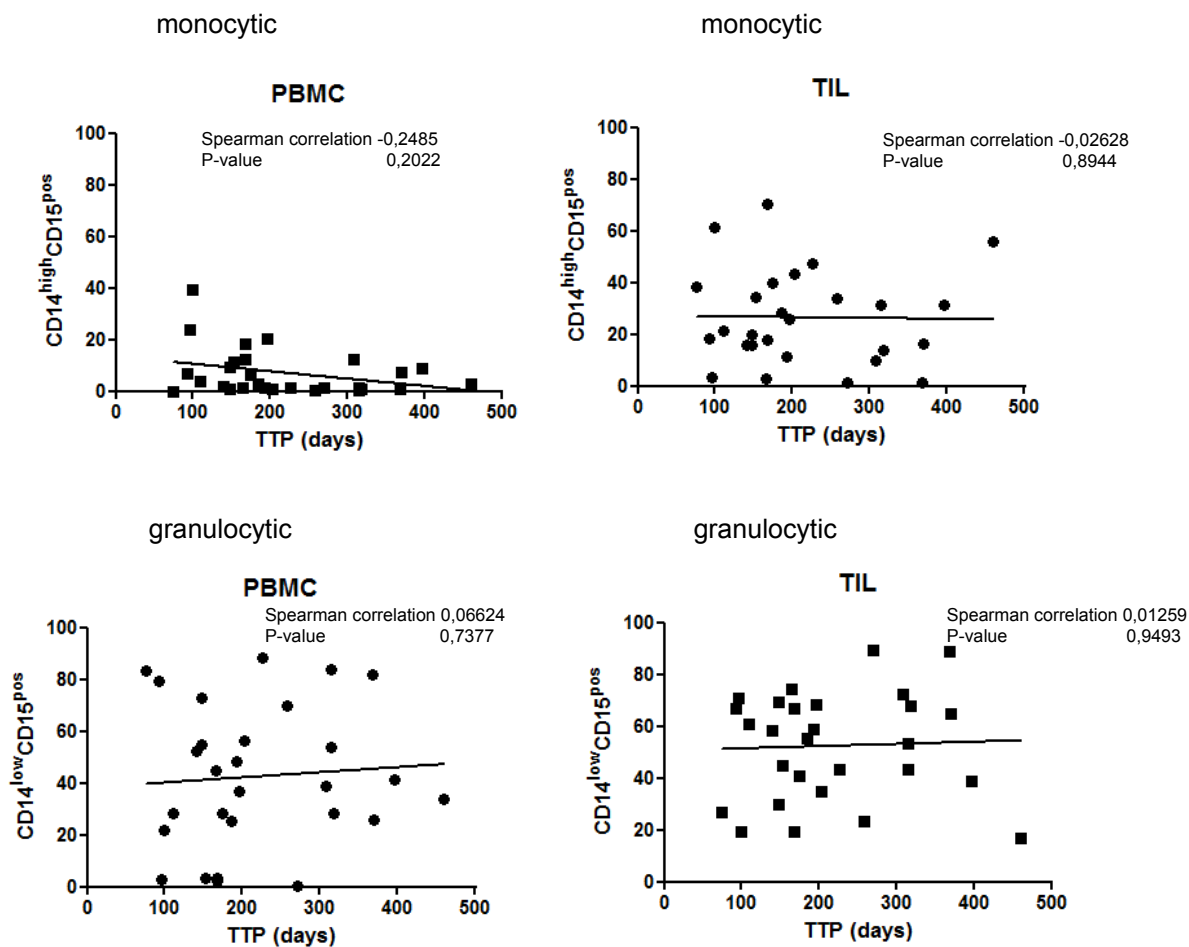


Figure20:Correlation between the proportion of monocyctic (CD14^{high}CD15^{positive}) or granulocytic (CD14^{low}CD15^{positive}) TIL and PBMC MDSCs and the time to progression (n=28).

5.Discussion

Myeloid-derived suppressor cells (MDSCs) comprise a heterogeneous population of myeloid cells, which are significantly expanded in cancer patients and are associated with tumor progression.

This study gives a detailed characterization of the frequency, phenotype and suppressive function of distinct MDSC subsets in peripheral blood and tumor tissue of a large cohort of patients with primary glioblastoma. In peripheral blood, it could be shown that both the proportion of CD14^{high}CD15^{positive} monocytic and CD14^{low}CD15^{pos} granulocytic MDSCs was significantly higher compared to healthy controls. The majority of granulocytic MDSCs consisted of CD14^{low}CD15^{positive} neutrophilic MDSCs.

In the tumor, a large proportion of CD14^{low}CD15^{positive} granulocytic MDSCs was found, that mainly consisted of neutrophilic CD14^{low}CD15^{high} MDSCs, but also an increased amount of CD14^{high}CD15^{positive} monocytic MDSCs. These findings are supported by recently published data from Raychaudhuri et al. who observed a predominance of granulocytic (CD15^{positive}CD14^{negative}) over monocytic (CD15^{negative}CD14^{positive}) MDSCs in tumor specimens of glioblastoma patients [41].

It was also analyzed whether the MGMT methylation status of the tumor or the use of corticosteroids influenced the frequency of MDSC subsets in blood and tumors, but we could not detect significant differences between tumors with an unmethylated or methylated MGMT status or steroid users and non-users in our large patient cohort. Noteworthy, the time of steroid ingestion before tumor resection was not analyzed. This could be a confounding factor since steroids could influence the MDSC frequency and phenotype.

Interestingly, the relative frequency of MDSC subsets was dependent on the tumor volume before resection with higher proportions of granulocytic MDSCs in larger tumors, whereas higher proportions of monocytic MDSCs were present in smaller tumors. Reasons for the positive correlation between tumor volume and MDSCs amount could be that a proportionally higher amount of tissue necrosis and hypoxia increases the production of chemo-attractants. The predomination of granulocytic MDSC within the tumor could be due to a selective chemokine-receptor expression

on different MDSCs subtypes. In this context, it would not only be interesting to analyze which chemokines are predominantly produced by glioblastomas depending on the tumor size, but also to get more information about the spatiotemporal distribution of these cells within the tumor. In a murine model, Sawanobori et al. showed that tumor-infiltrating neutrophils accumulate near the center of the tumor, whereas ARG1-expressing macrophages were distributed throughout the tumor mass [42]. After infiltrating into glioblastoma tissue, MDSCs are strongly modified by the tumor microenvironment. It could be seen that both granulocytic and monocytic MDSCs showed an activated phenotype with downregulation of CD16 and upregulation of HLA-DR, most prominent in monocytic MDSCs. While eosinophilic MDSCs also revealed strong upregulation of HLA-DR, neutrophilic MDSCs displayed a diverse HLA-DR expression pattern. Further subanalysis showed that HLA-DR^{low/-} neutrophilic MDSCs were CD16^{positive}, expressed CD124 and were Arginase I positive, whereas HLA-DR^{positive} neutrophilic MDSCs were CD16^{negative}, did not express CD124 and were Arginase I negative (data not shown). This also suggests that there is an enormous plasticity within the granulocytic fraction of MDSCs within glioblastomas. Monocytic MDSCs were strongly positive for CD124 and Arginase I, in contrast to their counterparts in peripheral blood. These cells also strongly expressed CD206 and the GM-CSF receptor (data not shown) and thus might correspond to the population of previously described tumor-associated macrophages (TAM) displaying a M2 phenotype [43]. Recently, Kohanbash et al. showed that CD124 mediates the IL-13-induced production of Arginase within bone marrow-derived myeloid cells which suppressed T-cell proliferation in an IL-4R α -dependent manner [44]. They also identified a fraction of CD33⁺CD14⁺HLADR⁻ cells within glioblastomas that expressed CD124 and suppressed the proliferation of autologous CD8⁺ T-cells.

This study also adds insight into the contribution of different MDSC subsets to the inhibition of T-cell activity in peripheral blood and tumor tissue. It could be observed that mainly freshly isolated blood-derived neutrophilic and less effectively eosinophilic MDSCs, but not monocytic MDSCs were able to suppress autologous non-specific T-cell proliferation and IFN- γ secretion in vitro. This is in accordance with previous reports demonstrating that peripheral cellular immunosuppression in patients with glioblastoma is mediated by degranulated neutrophils or CD33⁺CD15⁺ cells [27, 45]. Altogether, these results clearly demonstrate that granulocytic MDSCs are the

functionally immunosuppressive subset in the blood of glioblastoma patients. In contrast, freshly isolated tumor-derived MDSCs did not show T-cell inhibitory capacities in our standard T-cell suppression assay. Similar observations have been made by Gros et al. in patients with metastatic melanoma [46]. They speculated that HLA-DR expression on MDSCs distinguishes T-cell suppressive from non-suppressive cells. Our preliminary experiments with anti-HLA blocking monoclonal antibodies did not lead to different results suggesting that HLA-DR expression is not a decisive factor (data not shown). Although it is shown that tumor-derived MDSCs express significant amounts of Arginase I, our findings do not rule out that tumor-derived MDSCs are able to suppress T-cell functions in vivo, because our T-cell suppression assay with a coculture time of more than 96 hours might not reflect the immediate suppressive capacity of tumor-derived MDSCs or tumor-specific co-factors that are essential for the release of Arginase I containing granules from tumor-derived MDSCs into the culture supernatant are missing [47]. Finally, it could not be fully excluded that the isolation procedure of MDSCs from tumor tissue affects their suppressive capacity subsequently in vitro analysis.

As regulatory T-cells (Treg) play an important role in GBM-induced immunosuppression, it was interesting to see whether there was a relationship between MDSCs subsets and Treg at the tumor site. As shown in Figure 19. significant correlations between MDSC subsets and tumor-infiltrating Treg could not be found. However, this finding does not rule out the possible interaction between other T-cell subpopulations and their functioning inside tumor microenvironment. Finally, it was investigated whether there was a positive association between the frequency of different MDSC subsets in peripheral blood or tumor tissue and the time of tumor progression of glioblastoma. No significant correlation was found between the frequency of different MDSC subsets and time to tumor progression (TTP). This could be explained by the heterogeneity of the tumors and different responses to subsequent radiation and chemotherapy.

In summary, this thesis has several clinical implications for immune-based interventions in glioblastomas. First, as the tumor size strongly correlates with the accumulation of MDSCs at the tumor site, tumor reduction should be as good as possible to achieve a minimal residual disease status which is one of the prerequisites for an effective immunotherapy [48]. Secondly, strategies to target

MDSCs in peripheral blood and tumor tissue should be implemented into immunotherapeutic approaches, because MDSCs comprise the most prominent cell type with immunosuppressive functions in peripheral blood and tumor tissue of glioblastomas. Several compounds including conventional chemotherapeutic drugs have been identified that can influence MDSCs at different levels of [49].

These findings give new insight into the immunobiology of GBM, providing a detailed characterization of the nature and suppressive function of MDSCs in GBM patients and its clinical implication for immune based interventions in glioblastomas. First, granulocytic MDSCs in peripheral blood and tumor tissue should be carefully monitored during immunotherapeutic studies in glioblastoma patients. Second, strategies to target MDSCs in peripheral blood and tumor tissue should be implemented into immunotherapeutic approaches, because MDSCs comprise the most prominent cell types with immunosuppressive functions in peripheral blood and tumor tissue of glioblastoma patients.

6. Summary

Myeloid-derived suppressor cells (MDSCs) comprise a heterogeneous population of myeloid cells that are significantly expanded in cancer patients and are associated with tumor progression. Multicolor flow cytometry was used to study the frequency, phenotype, and function of MDSCs in peripheral blood and freshly resected tumors of 52 participants with primary glioblastoma (GBM). The frequency of CD14^{high}CD15^{positive} monocytic and CD14^{low}CD15^{positive} granulocytic MDSCs was significantly higher in peripheral blood of GBM participants compared with healthy donors. The majority of granulocytic MDSCs consisted of CD14^{low}CD15^{high} neutrophilic MDSCs with high T-cell suppressive capacities. At the tumor side, an increase in CD14^{high}CD15^{positive} monocytic MDSCs and high frequencies of CD14^{low}CD15^{positive} granulocytic MDSCs was found, that displayed an activated phenotype with downregulation of CD16 and upregulation of HLA-DR molecules, which did not inhibit T-cell proliferative responses in vitro. Surprisingly neither the MGMT methylation status of the tumor tissue nor the use of steroids did influence the frequency of MDSC subsets in peripheral blood and tumors. Interestingly, the relative frequency of both MDSC subsets was dependent on the tumor volume before resection with higher proportions of granulocytic MDCs in larger tumors, whereas higher proportions of monocytic MDCs were present in smaller tumors. This thesis provide a detailed characterization of different MDSC subsets in GBM patients and indicate that both granulocytic MDSCs in peripheral blood and at the tumor site play a major role in GBM-induced T-cell suppression.

7. Zusammenfassung

Myeloiden Suppressorzellen (MDSC) wird eine zentrale Rolle bei der Immunsppression in malignen Gliomen zugeschrieben. In der vorliegenden Arbeit wurde die Frequenz, der Phänotyp und die suppressive Funktion von MDSC im peripheren Blut und im Tumorgewebe von insgesamt 52 Patienten untersucht.

Die Analyse zeigte, dass der Anteil an $CD14^{high}CD15^{positive}$ (monozytärer Phänotyp) und der $CD14^{low}CD15^{positive}$ (granulozytärer Phänotyp) MDSCs im peripheren Blut von Glioblastompatienten im Vergleich zu Kontrollpersonen stark erhöht ist. Die Mehrheit des granulozytären Phänotyps besteht aus $CD14^{low}CD15^{high}$ (Neutrophiler Phenotyp) MDSCs, die eine hohe Immunosuppressivität aufzeigten.

Im Tumorgewebe konnte eine Erhöhung der $CD14^{high}CD15^{positive}$ MDSCs sowie der $CD14^{low}CD15^{positive}$ MDSCs nachgewiesen werden. Desweiteren zeigte sich eine Herunterregulierung von CD16 und einer Aufregulierung von HLA-DR der MDSCs im Tumorgewebe, welche auf einen aktivierten Phänotypen hindeutete. Bemerkenswerterweise korrelierte weder der MGMT Promotor-Methylierungsstatus noch die Einnahme von Steroiden mit dem Auftreten der Häufigkeit von MDSCs im periphären Blut noch im Tumorgewebe. Darüber hinaus konnte ein höheres Auftreten von granulozytären MDSCs in Tumoren größeren Volumens nachgewiesen werden, wo hingegen Tumore kleineren Volumens einen höheren Anteil an monozytären MDSCs aufzeigten. Die hier vorliegende Arbeit zeigt eine ausführliche Charakterisierung der verschiedenen MDSC Subtypen in Glioblastompatienten. Es konnte gezeigt werden, dass dem granulozytären MDSC Phänotyp sowohl im Blut als auch im Tumorgewebe die führende Rolle in der MDSC induzierten T-Zell Immunosuppression zukommt.

8. References

- [1] Weller, M., Tonn, J., Ernemann, U., Wiestler, O. and Bamberg, M. 2009. Glioblastome – Aktuelle Standards bei Diagnostik und Therapie. *Best Practice Onkologie*, 4(2), 4-11.
- [2] Wen, P.Y. and Kesari, S. 2008. Malignant gliomas in adults. *NEJM*, 359(5), 492-507.
- [3] Kleihues, P. and Ohgaki, H. 1999. Primary and secondary glioblastomas: From concept to clinical diagnosis. *J Neuropathol Exp Neurol*. 2005 Jun;64(6):479-89.
- [4] Louis, D.N., Ohgaki and H., Wiestler, O.D. 2007. The 2007 WHO Classification of Tumours of the Central Nervous System. *Acta Neuropathologica* 2007. 114:97-109.
- [5] Ahmed, R., Oborski, M., Hwang, M., Lieberman, F and Mountz, J. 2014. Malignant gliomas: current perspectives in diagnosis, treatment, and early response assessment using advanced quantitative imaging methods. *Cancer Manag Res*. 2014; 6: 149–170.
- [6] Whittle, I.R., Pringle, A.M. and Taylor, R. 1998. Effects of resective surgery for leftsided intracranial tumours on language function: a prospective study. *Lancet*. 1998 Apr 4;351(9108):1014-8.
- [7] Stewart, L.A.. 2002. Chemotherapy in adult high-grade glioma: a systematic review and meta-analysis of individual patient data from 12 randomised trials. *Lancet* 2002;359:1011-8.
- [8] Jackson, R.J., Fuller, G.N., Abi-Said, D., Lang, F.F., Gokaslan, Z.L. and Shi, W.M. 2001. Limitations of stereotactic biopsy in the initial management of gliomas. *Neuro-oncol* 2001;3:193-200.
- [9] Stummer, W., Pichlmeier, U., Meinel, T., Wiestler, O.D., Zanella, F., Reulen, H.J. and ALA-Glioma Study Group. 2006. Fluorescence-guided surgery with 5-aminolevulinic acid for resection of malignant glioma: a randomised controlled multicentre phase III trial. *Lancet Oncol*. 2006 May;7(5):392-401.
- [10] Stupp, R., Hegi, M.E., Mason, W.P., van den Bent, M.J., Taphoorn, M.J., Janzer, R.C., Ludwin, S.K., Allgeier, A., Fisher, B., Belanger, K., Hau, P., Brandes, A.A., Gijtenbeek, J., Marosi, C., Vecht, C.J., Mokhtari, K., Wesseling, P., Villa, S., Eisenhauer, E., Gorlia, T., Weller, M., Lacombe, D., Cairncross, J.G., Mirimanoff, R.O., European Organisation for Research and Treatment of Cancer Brain Tumour and Radiation Oncology Groups and National Cancer Institute of Canada

- ClinicalTrials Group. 2009. Effects of radiotherapy with con-comitant and adjuvant temozolomide versus radiotherapy alone on survival in glioblastoma in a randomised phase III study: 5-year analysis of the EORTC-NCIC trial. *Lancet Oncol.* 2009 May;10(5):459-66.
- [11] Stupp, R., Hegi, M., van den Bent, M., Mason, W., Weller, M., Mirimanoff, R. and Cairncross, G., 2006. Changing Paradigms—An Update on the Multidisciplinary Management of Malignant Glioma. *The Oncologist February 2006 Vol.11, Issue 2 page 165-180.*
- [12] Liu, W., Putman, A.L., Xu-you, Z., Szot, G.L., Lee, M.R., Zhu, S., Gottlieb, P.A., Kapranov, P., Gingeras, T.R., Fazekas, de St., Groth, B., Clayberger, C., Soper, D.M., Ziegler, S.F. and Bluestone, J.A. 2006. CD127 expression inversely correlates with FoxP3 and suppressive function of human CD4+ T reg cells. *The Journal of Experimental Medicine*, 203(7), 1701-1711.
- [13] Murphy, K.M., Travers, P. and Walport, M. 2009. Janeway Immunologie. Spektrum Verlag.
- [14] Hori, S., Nomura, T. and Sakaguchi, S. 2003. Control of regulatory T cell development by the transcription factor Foxp3. *Science*, 299, 1057-1061.
- [15] Vignali, L. W., Collison, L. W. and Workman, C. J. 2008. How regulatory T cells work. *Nat Rev Immunol.* 2008 July ; 8(7): 523–532.
- [16] Walker, P.R., Calzascia, T. and Dietrich, P.Y. 2002. All in the head: obstacles for immune rejection of brain tumours. *Immunology*, 107, 28-38.
- [17] Friese, M.A., Steinle, A. and Weller, M. 2004. The innate immune response in the central nervous system and its role in glioma immune surveillance. *Onkologie*, 27, 487- 491.
- [18] Appay, V., Dunbar, P.R., Callan, M., Klenerman, P., Gillespie, G.M., Papagno, L., Ogg, G.S., King, A., Lechner, F., Spina, C.A., Little, S., Havlir, D.V., Richman, D.D., Gruener, N., Pape, G., Waters, A., Easterbrook, P., Salio, M., Cerundolo, V., McMichael, A.J., Hickey, W.F. 1991. Migration of hematogenous cells through the blood-brain barrier and the initiation of CNS inflammation. *Brain Pathology*, 1(2), 97-105.
- [19] Louveau, A., Smirnov, I., Keyes, T.J., Eccles, J.D., Rouhani, S.J., Peske, J.D., Derecki, N.C., Castle, D., Mandell, J.W., Lee, K.S., Harris, T.H. and Kipnis, J. 2015. Structural and functional features of central nervous system lymphatic vessels. *Nature*. 2015;523(7560):337-341.

- [20] Cserr, H.F., DePasquale, M., Harling-Berg, C.J., Park, J.T. and Knopf P.M. 1992. Afferent and efferent arms of the humoral immune response to CSF-administered albumins in a rat model with normal blood-brain barrier permeability. *Journal of Neuroimmunology*, 41(2), 195-202.
- [21] Bradl, M. and Hohlfeld, R. 2003. Molecular pathogenesis of neuroinflammation. *J Neurol Neurosurg Psychiatry*, 74, 1364-1370.
- [22] Grauer, O.M., Wesseling, P., Adema, G.J. 2009. Immunotherapy of Diffuse Gliomas: Biological Background, Current Status and Future Developments. *Brain Pathol.* 2009;19(4):674-693.
- [23] Jacobs, J.F., Idema, A.J., Bol, K.F., Nierkens, S., Grauer, O.M., Wesseling, P., Grotenhuis, J.A., Hoogerbrugge, P.M., de Vries, I.J. and Adema, G.J. 2009. Regulatory T cells and the PD-L1/PD-1 pathway mediate immune suppression in malignant human brain tumors. *Neuro Oncol.* 2009 Aug;11(4):394-402.
- [24] Youn, J.I., Nagaraj, S., Collazo, M. and Gabrilovich, D.I. 2008. Subsets of myeloid-derived suppressor cells in tumor-bearing mice. *J Immunol*, 2008. 181(8): p. 5791-802.
- [25] Hanson, E.M., Clements, V.K., Sinha, P., Ilkovitch, D. and Ostrand-Rosenberg, S. 2009. Myeloid-DerivedSuppressor Cells Down Regulate L-Selectin Expression on CD4+ and CD8+ T Cells. *JImmunol.* 2009;183(2):937-944.
- [26] Dilek, N., de Sully, R.V., Blanco, G. and Vanhove, B. 2012. Myeloid-derived suppressor cells: Mechanisms of action and recent advances in their role in transplant tolerance. *Front Immunol.* 2012;3(JUL):1-9.
- [27] Raychaudhuri, B., Rayman, P., Ireland, J., Ko, J., Rini, B., Borden, E.C., Garcia, J., Vogelbaum, M.A. and Finke, J. 2011. Myeloid-derived suppressor cell accumulation and function in patients with newly diagnosed glioblastoma. *Neuro Oncol* 2011;13(6):591-599.
- [28] Parker, K.H., Beury, D.W. and Ostrand-Rosenberg, S. 2015. Myeloid-Derived Suppressor Cells: Critical Cells Driving Immune Suppression in the Tumor Microenvironment. *Adv Cancer Res.* 2015;128:95-139.
- [29] Hermiston, M.L., Zikherman, J. andZhu, J.W. 2009. CD45, CD148, and Lyp/Pep: critical phosphatases regulating Src family kinase signaling networks in immune cells“. *Immunol Rev.* 2009 Mar;228(1):288-311.
- [30] Kannagi, R., Mitsuoka, C., Kawakami-Kimura, N., Kasugai-Sawada, M.,

- Hiraiwa, N., Toda, K., Ishida, H., Kiso, M., Hasegawa, A. and Kannagi, R. 1997. Sulfated sialyl Lewis X, the putative L-selectin ligand, detected on endothelial cells of high endothelial venules by a distinct set of anti-sialyl Lewis X antibodies. *Biochem Biophys Res Commun* 1997 Apr 17;233(2):576.
- [31] Greten, T.F., Manns, M.P. and Korangy F. 2011. Myeloid derived suppressor cells in human diseases.“ *Int Immunopharmacol. Int Immunopharmacol.* 2011 Jul;11(7):802-7.
- [32] Filipazzi, P., Huber, V. and Rivoltini, L. 2012. Phenotype, function and clinical implications of myeloid-derived suppressor cells in cancer patients. *Cancer Immunol Immunother.* 2012 Feb;61(2):255-63.
- [33] Diaz-Montero, C.M., Salem, M.L., Nishimura, M.I., Garrett-Mayer, E., Cole, D.J. and Montero, A.J. 2009. Increased circulating myeloid-derived suppressor cells correlate with clinical cancer stage, metastatic tumor burden, and doxorubicin-cyclophosphamide chemotherapy. *Cancer Immunol Immunother.* 2009, Jan;58(1):49-59.
- [34] Rodriguez, P.C., Ernstoff, M.S., Hernandez, C., Atkins, M., Zabaleta, J., Sierra, R. and Ochoa, A.C. 2009. Arginase I-producing myeloid-derived suppressor cells in renal cell carcinoma are a subpopulation of activated granulocytes. *Cancer Res.* 2009 Feb 15;69(4):1553-60.
- [35] Hoechst, B., Ormandy, L.A., Ballmaier, M., Lehner, F., Krüger, C., Manns, M.P., Greten, T.F. and Korangy, F. 2008. A new population of myeloid-derived suppressor cells in hepatocellular carcinoma patients induces CD4(+)CD25(+)Foxp3(+) T cells. *Gastroenterology.* 2008 Jul;135(1):234-43.
- [36] Chien-Ying, L., Liu, C.Y., Wang, Y.M., Wang, C.L., Feng, P.H., Ko, H.W., Liu, Y.H., Wu, Y.C., Chu, Y., Chung, F.T., Kuo, C.H., Lee, K.Y., Lin, S.M., Lin, H.C., Wang, C.H., Yu, C.T. and Kuo, H.P. 2010. Population alterations of L-arginase- and inducible nitric oxide synthase-expressed CD11b+/CD14⁺/CD15+/CD33⁺ myeloid-derived suppressor cells and CD8⁺ T lymphocytes in patients with advanced-stage non-small cell lung cancer. *J Cancer Res Clin Oncol* (2010) 136:35–45.
- [37] Mundy-Bosse, B.L., Lesinski, G.B., Jaime-Ramirez, A.C., Benninger, K., Khan, M., Kuppusamy, P., Guenterberg, K., Kondadasula, S.V., Chaudhury, A.R., La Perle, K.M., Kreiner, M., Young, G., Guttridge, D.C. and Carson, W.E. 2011. 3rd. Myeloid-derived suppressor cell inhibition of the IFN response in tumor-bearing mice. *Cancer Res.* 2011 Aug 1;71(15):5101-10.
- [38] Vuk-Pavlović, S., Bulur, P.A., Lin, Y., Qin, R., Szumlanski, C.L., Zhao, X. and Dietz, A.B. 2010. Immunosuppressive CD14+HLA-DR^{low}/- monocytes in prostate

cancer. *Prostate*. 2010 Mar 1;70(4):443-55.

[39] Gabrilovic, I.D. and Nagaraj S. 2009. *Nature review immunology 2009, Vol. 9 Issue 3, page 162-174.*

[40] Flamm, E.S., Ransohoff, J., Wuchinich, D. and Broadwin, A. 1978. Preliminary experience with ultrasonic aspiration in neurosurgery. *Neurosurgery*. 2(3): 240-245.

[41] Raychaudhuri, B., Rayman, P., Huang, P., Grabowski, M., Hambardzumyan, D., Finke, J.H. and Vogelbaum, M.A. 2015. Myeloid derived suppressor cell infiltration of murine and human gliomas is associated with reduction of tumor infiltrating lymphocytes. *J. Neurooncology 2015; 122(2): 293-301.*

[42] Sawanobori, Y., Ueha, S., Kurachi, M., Shimaoka, T., Talmadge, J.E., Abe, J., Shono, Y., Kitabatake, M., Kakimi, K., Mukaida, N. and Matsushima, K. 2008. Chemokine-mediated rapid turnover of myeloid-derived suppressor cells in tumor-bearing mice. *Blood 2008;111(12):5457-66.*

[43] Umemura, N., Saio, M., Suwa, T, Kitoh, Y., Bai, J., Nonaka, K., Ouyang, G.F., Okada, M., Balazs, M., Adany, R., Shibata, T. and Takami, T. 2008. Tumor-infiltrating myeloid-derived suppressor cells are pleiotropic-inflamed monocytes/macrophages that bear M1- and M2-type characteristics. *J Leukoc Biol*. 2008; 83(5):1136-1144.

[44] Kohanbash, G., McKaveney, K., Sakaki, M., Ueda, R., Mintz, A.H., Amankulor, N., Fujita, M., Ohlfest, J.R. and Okada, H. 2013. GM-CSF promotes the immunosuppressive activity of glioma-infiltrating myeloid cells through interleukin-4 receptor-alpha. *Cancer Res*. 2013; 73(21):6413-6423.

[45] Sippel, T.R., White, J., Nag, K., Tsvankin, V., Klaassen, M., Kleinschmidt-DeMasters, B.K. and Waziri, A. 2011. Neutrophil degranulation and immunosuppression in patients with GBM: restoration of cellular immune function by targeting arginase I. *Clin Cancer Res*. 2011; 17(22):6992-7002.

[46] Gros, A., Turcotte, S., Wunderlich, J.R., Ahmadzadeh, M., Dudley, M.E. and Rosenberg, S.A. 2012. Myeloid cells obtained from the blood but not from the tumor can suppress T-cell proliferation in patients with melanoma. *Clin Cancer Res* 2012;18(19):5212-23.

[47] Haverkamp, J.M., Crist, S.A., Elzey, B.D., Cimen, C. and Ratliff, T.L. 2011. In vivo suppressive function of myeloid-derived suppressor cells is limited to the inflammatory site. *Eur J Immunol*. 2011; 41(3):749-759.

[48] Rutkowski, S., De Vleeschouwer, S., Kaempgen, E., Wolff, J.E., Kuhl, J., Demaerel, P., Warmuth-Metz, M., Flamen, P., Van Calenbergh, F., Plets, C.,

Sørensen, N., Opitz, A. and Van Gool, S.W. 2004. Surgery and adjuvant dendritic cell-based tumour vaccination for patients with relapsed malignant glioma, a feasibility study. *Br J Cancer* 2004;91(9):1656-62.

[49] Ugel, S., Delpozzi, F., Desantis, G., Papalini, F., Simonato, F., Sonda, N., Zilio, S. and Bronte, V. 2009. Therapeutic targeting of myeloid-derived suppressor cells. *Curr Opin Pharmacol* 2009;9(4):470-81.

Acknowledgements

Mein herzlicher Dank gilt:

Meinen Eltern und ärztlichen Kollegen **Marina Dubinski** und **Michael Geuchmann** sowie meiner lieben Schwester **Lena Dubinski**.

Die Unterstützung und Liebe meiner Ehefrau **Sarah Dubinski** trägt mich jeden Tag.

Priv.-Doz. Dr. Dr. med. Oliver M. Grauer für die hervorragende Betreuung, die Unterstützung, Förderung und Hilfe bei dem Verfassen dieser Arbeit.

Prof. Dr. med. Ulrich Bogdahn für die Möglichkeit, die Arbeit an der von ihm geleiteten Klinik und Poliklinik für Neurologie der Universität Regensburg durchzuführen.

Prof. Dr. med. Peter Hau für seine Unterstützung und hilfreichen Beiträge sowie das zur Verfügung stellen von Labor und Material.

Dr. rer. nat. Sridhar Chirasani danke ich als Ansprechpartner für die vielen Techniken und theoretischen sowie praktischen Grundlagen die ich durch Ihn erlernen konnte.

Ilja Dubinski der mir als Bruder, Freund und ärztlicher Kollege unersetzlich wichtig ist.

Prof. Dr. med. Oliver Habler für die Unterstützung in meinen ersten universitären Schritten.

Priv.-Doz. Dr. med. Kartik Krishnan für seine persönliche wie fachliche Kompetenz und seinen Glauben an mich.

Dr. med. Heinke Hardung und **Dr. med. Christoph Hardung** die mich als Schwiegereltern und Kollegen stets unterstützt haben.

Curriculum Vitae

Name: Daniel Dubinski M.Sc.
Geburtsdatum, - ort: 21.03.1985 in Moskau
Staatsangehörigkeit: deutsch
Familienstand: verheiratet
Anschrift: Stegstr.34
60594 Frankfurt am Main
Telefon 0176/70196014
Email: danieldubinski@gmail.com



Akademischer/Beruflicher Werdegang

Seit 03/2015 Assistenzarzt Klinik und Poliklinik für Neurochirurgie,
Universitätsklinikum Frankfurt, Direktor: Prof. Dr. V. Seifert

2012-2014 Masterstudiengang „Experimental and Clinical Neurosciences“,
Elite Netzwerk Bayern, Universität Regensburg

2009-2014 Studium der Humanmedizin, Universität Regensburg

2007 - 2009 Studium der Humanmedizin, Universität Pécs (Ungarn)

1998 Abitur, Klinger Gymnasium Frankfurt

Auslandsaufenthalte

2014 Clinical Fellowship: Weill Cornell Medical College, New York
Presbyterian Hospital, Department of Vascular Surgery,
Director: D. B. Schneider, M.D.

2014 Clinical Fellowship: Weill Cornell Medical College, New York
Presbyterian Hospital, Department of Pediatric Surgery,
Director: N.A. Spigland, M.D.

Lehrerfahrung

2009/2011 Hilfwissenschaftler am Institut für Zelluläre und Molekulare
Anatomie im Kurs Neuroanatomie der Universität Regensburg
Leitung: Prof. Dr. R. Witzgall

Auszeichnungen

2011 Deutschlandstipendium, Bundesministerium für Bildung und
Forschung

Regensburg, den 17.03.2016

ERKLÄRUNG ZUM PROMOTIONSVERFAHREN

nach § 3 Abs. 3 und 4 der Promotionsordnung
der Fakultät für Medizin der Universität Regensburg

Name: _____

Vorname: _____

geb. am: _____

in: _____

Ich erkläre,

- dass ich den **Doktorgrad der Medizin / Zahnheilkunde*** nicht schon an einer Hochschule der Bundesrepublik Deutschland erworben habe
- dass ich nicht an anderer Stelle zu einem Promotionsverfahren zum Erwerb des **medizinischen / zahnmedizinischen Doktorgrades*** zugelassen bin
- dass ich die **medizinische / zahnmedizinische Doktorprüfung*** nicht schon an einer Hochschule der Bundesrepublik Deutschland endgültig nicht bestanden habe

Außerdem erkläre ich,

- dass mir keine Tatsachen bekannt sind, die mich zur Führung eines akademischen Grades im Sinne des Gesetzes über die Führung akademischer Grade unwürdig erscheinen lassen
- dass ich die vorliegende Arbeit ohne unzulässige Hilfe Dritter und ohne Benutzung anderer als der angegebenen Hilfsmittel angefertigt habe. Die aus anderen Quellen direkt oder indirekt übernommenen Daten und Konzepte sind unter Angabe der Quelle gekennzeichnet. Insbesondere habe ich nicht die entgeltliche Hilfe von Vermittlungs- bzw. Beratungsdiensten (Promotionsberater oder andere Personen) in Anspruch genommen. Niemand hat von mir unmittelbar oder mittelbar geldwerte Leistungen für Arbeit erhalten, die im Zusammenhang mit dem Inhalt der vorgelegten Dissertation stehen. Die Arbeit wurde bisher weder im In- noch im Ausland in gleicher oder ähnlicher Form einer anderen Prüfungsbehörde vorgelegt.

(Ort, Datum)

(Unterschrift)

Die einmalige Rücknahme des Promotionsgesuches ist bis zur Bestellung der Gutachter zulässig.

* Nicht Zutreffendes bitte streichen